

Corrosion behavior of 304 stainless steel in borate buffer solution: effects of pH & chloride ions

*Thesis submitted in partial fulfillment
of the requirements of the degree of
Master of Technology*

in

*Mechanical Engineering
(Steel Technology)*

by

Pundrikaksha Upadhyay

(Roll Number: 214MM2506)

under the supervision of

Prof. Archana Mallik



Department of Metallurgical and Materials Engineering

National Institute of Technology, Rourkela-769008

Odisha, India

May2016

Dedicated to,

My Parents



**Department of Metallurgical and Materials
Engineering, National Institute of Technology,
Rourkela – 769008, Odisha,
India**

CERTIFICATE

This is to certify that the thesis entitled “**Corrosion behavior of 304 stainless steel in borate buffer solution: effects of pH & chloride concentration**” submitted by **Pundrikaksha Upadhyay** to National Institute of Technology, Rourkela is a record of bonafide research work under our supervision and is worthy of consideration for the award of the degree of M. Tech of the Institute. The candidate has fulfilled all prescribed requirements for the thesis, which is based on candidate’s own work, has not been submitted elsewhere for a degree or diploma.

Prof. Archana Mallik
Supervisor
Assistant Professor

Acknowledgment

This project was carried out at National Institute of Technology, Rourkela under a span of 2 years, which undertook a lot of effort and help from different persons, without whom this research work wouldn't have been as fruitful as it is, and I would like to extend my deepest gratitude to all of them for making me what I am today.

First of all, my supervisor, Prof. Archana Mallik, as dynamic as is her personality, she is one of the kind hearted person I have ever met. Her need to keep me innovative and punctual had brought in me vivid changes which I will explore throughout my life, She is what we say the teacher of “Modern times”, unravelling in me the science. Madam, I have been a little insincere and casual yet you have been patient, you made me realise the importance of little things, significance of literature and design in technology and of all to be patient. From the core of my heart, I would like to thank you, for your constant support and encouragement and I really look forward to work with you in the near future.

I am grateful to Dr. C. K. Behera for his supervision and support in carrying out this project in IIT-BHU.

I would like to thank the laboratory members of Department of Metallurgical and Materials Engineering and Central Workshop, NIT Rourkela.

Now to the members of our lab, Sumanta Kumar, Ramkumar, Akhya Behera, Prekshya Nath, Deepak Sahu, Duleshwar Singh guys talking to you all was a family of garden, you were always there, alleviating the pressure of the rigorous work. Thank you all!! It was a time well spent.

I would like to say special thanks my parents, friends and other members of department who have always been supporting me in my studies. Thanks for your love and support!

All errors and limitations remaining in this thesis are mine alone.

Pundrikaksha Upadhyay

(May 2016)

Abstract

The thin adherent oxide layer formed on the metal surface keeps the surface of metal protective from corrosion i.e. known as passivation. This oxide layer may break due to different types of environmental effects leading to rapid corrosion. Hence the study on breakdown of passivity should permit one for the interpretation of process parameter and environmental restriction for long time of serviceable of the metal. The 304 stainless steel is having the higher percentage of chromium making it corrosion proof literally. In this thesis the study is on the passivity breakdown of 304 stainless steel in deaerated borate buffer solution as a function of pH and Cl ions. The pitting corrosion studies of 304 SS is carried out in borate buffer solution at varying pH (8.3,9.3,10.3) in the presence of varying chloride ions (0.1M, 0.5M, 1M). Corrosion studies were performed by potentiodynamic scans, microscopy techniques and point defect model. The study of the passivity and pitting can be evaluated through a point defect model. As increasing the pH of borate buffer solution, the breakdown potential increases i.e. the pitting tendency decreases whereas it got decreased with increasing chloride ion concentration.

The value of breakdown potential was also found to increase with the potential scan rate. After obtaining the potentiodynamic curve pitting studies of the surface is done by optical microscope. The microstructure is shown in above figure at 1M chloride ion and at varying pH. The probability distribution in breakdown potential is the confirmation with the analytical prediction of the breakdown potential distribution obtained from the point defect model.

Keywords: Passivation, breakdown potential, borate buffer solution, 304 steel, PDM

Contents

<i>CERTIFICATE</i>	<i>iv</i>
<i>Acknowledgment</i>	<i>v</i>
<i>Abstract</i>	<i>vi</i>
<i>Nomenclature</i>	<i>vii</i>
<i>List of figures</i>	<i>viii</i>
<i>List of tables</i>	<i>x</i>
Chapter1	1
Introduction	1
1.1 Background	1
1.2 Research motivation	2
1.3 Objectives.....	2
1.4 Structure of the thesis	3
Chapter 2	4
Literature Review	4
2.1 Corrosion	4
2.2 Forms of Corrosion	4
2.2.1 Uniform Corrosion	4
2.2.2 Galvanic Corrosion	5
2.2.3 Crevice Corrosion	6
2.2.4 Pitting Corrosion	6
2.2.4 Intergranular corrosion	7
2.2.6 Hydrogen damage	8
2.2.7 Erosion Corrosion and Fretting	8
2.3 Steel	9
2.3.1 304 Stainless steel	10
2.3.2 316 stainless steel	12
2.4 Pitting Corrosion.....	13
2.4.1 Mechanism of pitting corrosion	14
2.5 Initiation and growth	18

2.5.1 Point Defect Model (PDM)	18
2.6 Passivity	21
2.7 Passivity breakdown	22
2.8 Summary	26
Chapter 3	27
Materials & Methods.....	27
3.1 Sample preparation	27
3.2 Solution preparation	28
3.3 Electrochemical Setup	29
3.5 Optical microscope.....	30
3.6 Electrochemical Measurements	30
Chapter 4	31
Results and Discussions.....	31
4.1 Passivity studies of 304 stainless steel.....	31
4.2 Breakdown potential for 304 stainless steel at room temperature	32
4.2.1 Distribution of breakdown potential and its calculation	35
4.3 Microstructural analysis of pitting corrosion on 304 stainless steel.....	43
Chapter 5	44
Conclusion	44
5.1 Summary.....	44
References.....	45

Nomenclature

F	Faraday constant
R	Universal gas constant
T	Absolute Temperature
N_V	Avogadro's number
χ	The film layer stoichiometry
Ω	Molar volume of Fe_2O_3 per cation
D	The mean cation vacancy diffusivity
$\alpha,$	Potential dependence of $\phi_{f/s}$
$\varepsilon,$	The electric field strength
$\xi,$	The critical vacancy concentration
$J_m,$	The critical vacancy flux
β	pH dependence of $\phi_{f/s}$
ν	Scan rate
V_c	Breakdown potential
a_{Cl^-}	Chloride concentration
j	Current density
J_{ca}	Cationic flux
J_a	Anionic flux
n	Electrons
h	holes
$V_M^{x'}$	Cation vacancy
V_0''	Anion vacancy
M	Metal atom
v_m	Metal holes

Abbreviations

PDM	Point Defect Model
SCE	Saturated Calomel Electrode
WE	Working Electrode
CE	Counter Electrode
RE	Reference Electrode

List of figures

Figure No.	Caption	Page
2.1	Uniform corrosion	5
2.2	Galvanic corrosion	5
2.3	Crevice Corrosion	6
2.4	Pitting Corrosion	7
2.5	Intergranular Corrosion	7
2.6	Hydrogen Cracking	8
2.7	Erosion corrosion	9
2.8	Mechanism of localized corrosion developing on metal in a solution containing oxygen	14
2.9	Corrosion mechanism	15
2.10	Formation of pitting above E_{pit}	16
2.11	Pitting on iron	17
2.12	Pitting corrosion stages	17
2.13	Potential distribution across the metal/ barrier layer / solution interface	19
2.14	Generation-I Point defect model	23
2.15	Generation-II Point defect model	24
2.16	The breakdown of passive films on the basis of PDM	25

3.1	Steps used for sample preparation	27
3.2	Three electrode electrochemical setup	29
4.1	The curve for potentiodynamic polarization of 304 SS in buffer solution	31
4.2	Open circuit voltage for 304 SS in borate buffer solution	32
4.3	Curves for potentiodynamic polarization 304 stainless steel in varying chloride	33
4.4	Breakdown potential at scan rate= 1mV/s for 304 SS in borate buffer solution having pH=9.3 is a function of the chloride ion activity	33
4.5	Polarization curve shows the dependency of breakdown potential on scan rate	34
4.6	Potentiodynamic curve at pH=9.3 with scan rate 0.167 mV/s	36
4.7	Potentiodynamic curve at pH=9.3 with scan rate 1mV/s	37
4.8	Potentiodynamic curve at pH=9.3 with scan rate 5mV/s	37
4.9	Potentiodynamic curve at pH=9.3 with scan rate 10mV/s	38
4.10	Potentiodynamic curve at pH=9.3 with scan rate 50mV/s	39
4.11	Potentiodynamic curve at pH=9.3 with scan rate 100mV/s	39
4.12	Potentiodynamic curve at pH=10.3 with scan rate 1mV/s	40
4.13	Cumulative probabilities in the breakdown potential for 304 SS with varying chloride concentration at pH 9.3	41
4.14	Cumulative probabilities in the breakdown potential for 304 SS in borate buffer solution with varying chloride concentration at pH 10.3	41
4.15	The microstructure of stainless steel before and after adding NaCl in solution	43

List of tables

Table no	Caption	Page no
2.1	Composition of 304 stainless steel	10
2.2	Properties of 304 Stainless steel	12
2.3	Composition of 316 Stainless steel	13
3.1	Composition of buffer solution	28
4.1	Parameters used to find the cumulative probabilities in breakdown potential	42

Chapter1

Introduction

1.1 Background

Iron is one of the most useful material in terms of use and availability. Many complicated machines, infrastructures and parts of the machines are manufactured with the iron and steel. Some other material as chromium, nickel, zirconium having other properties i.e. found from their ores by using electrochemical technique. These metals are used in so many industries, as in automobile and aircraft industries. The discovery of steel was the history of development.

Now a days the iron and steel plays important role in this progressive world, steel is found from iron ore. Some other materials as chromium, aluminium, nickel which are mixed with iron ore and form the steel, having important role also. Nitrogen, phosphorus and sulfur are impurities which are removed from the iron at the time of steel making. And other alloying elements are used to produce different types of grade steel. After adding alloying element they prevent the steel from corrosion. They are known as corrosion resistive material. Due to this corrosion the word 'passivity' was introduced.

Passivity is the condition of corrosion resistance. Passivity is the formation of oxide layer forms a continuous film which prevents the metal from corrosion. The term passivity was introduced by Schonbein and its correct representation gave by Faraday. This passivity phenomena was understood with the electrochemical thermodynamic diagram by Pourbaix. When oxide layer forms after some time it breaks due to some chemical or physical environment. Once the layer breaks it faces again corrosion problem [1,32].

Different types of model has been discovered since 1930 by different scientists to represent the passivity and passivity breakdown. The point defect model is the best model to represent the

passivity and its breakdown which was fully developed up to 1990. The point defect model having three generation and removed the errors of the other two generation.

1.2 Research motivation

The stainless steel is generally used in domestic, agricultural, transport, chemical, pharmaceutical, oil/gas, medical, water and sewage treatment plant and to make the springs, fasteners etc. Now a days the stainless steel is using very widely, so this steel should be corrosion resistive.

The 304 stainless steel is more corrosion resistive with respect to normally carbon or alloy steel. On the basis of daily use the stainless steel makes to resist the corrosion. Due to the corrosion the human body may affected during accident through metal, if that metal made of corrosion resistive then the body will prevent from corrosive environment. So in surgical equipment the stainless steel used widely.

1.3 Objectives

The objectives of the corrosion study is try to predict and explain the pitting corrosion on the metal surface of the steel in terms of the point defect model in borate buffer solution at different pH (8.3, 9.3, 10.3) at various chloride (Cl^-) concentration (0.1M, 0.5M, 1M).

The aim of this study is:

- (i) To determine the passive region, passive layer thickness and current.
- (ii) To find the breakdown potential as pH function, potential sweep rate & chloride concentration.
- (iii) To determine the relationship between breakdown potential and chloride concentration and potential sweep rate in terms of point defect model to find the passivity breakdown parameters.
- (iv) To evaluate the capacity of PDM to represent the passivity breakdown.

The potentiodynamic curves were plotting at varying pH & chloride concentration (Cl^-) and slope of the curves used to find the different parameters as explained the point defect model. After obtaining the parameters, a modelling has been done to plot cumulative probability

distribution plot by point defect model which was differentiate with the obtained data. The similarities gave the idea about the PDM to evaluate the breakdown of passivity on 304 stainless steel in the buffer solution.

1.4 Structure of the thesis

There is 5 chapters in this thesis. Chapter 2 deals with the passivity and passivity breakdown and the concepts of passivity breakdown is described followed by the development and the PDM and the approach with which PDM defines breakdown of passivity on 304 stainless steel in electrolyte i.e. borate buffer solutions.

Chapter 3 defines the materials and methods, experimental aspects, which include the sample preparation by the polishing and solution preparation i.e. chloride containing borate buffer solution, experimental setup, different types of potentiodynamic curves with different pH, chloride concentration and scan rate (0.167, 1, 5, 10, 50, 100 mV/s). From the above experiments the obtained data is used for computational modelling.

The conclusions are obtained from the experiment like potential V/S current density plot with different chloride concentration in electrolyte and pH are explained in chapter 4. So many parameters were obtained from these curves, these parameters were used for computational modelling of the passivity breakdown. The cumulative probability distribution of breakdown potential determined from the experimental data and different with the curve obtained from the point defect model.

Chapter 2

Literature Review

2.1 Corrosion

Corrosion is destruction or degradation of metals or alloys in presence of any kind of chemical or physical environment. Corrosion is omnipresent, this cause heavy machinery failure, expensive maintenance, monetary losses. When chemical reactions occur with the surrounding environment then same amount of energy is released during the use of metal in its form. Therefore, corrosion is the existence of the tendency of the metal to return to its parent form, from which it was removed. Hence, corrosion is extractive metallurgy in reverse [2,33].

Corrosion can revealed itself in various ways with each having certain specific characteristics and property. In our daily life the metal rusting is general phenomena. Rusting of iron, greenish colour on copper pots, tin can become black due to corrosion. The scopes of corrosion lies to great extent and so many things destroy due to corrosion in large scale. In daily life so many economic losses comes due to corrosion[1].

2.2 Forms of Corrosion

Different types of corrosion are given below[2,3],.

2.2.1 Uniform Corrosion

It is a type of corrosion attack (decay of the metal) that may be more or less uniformly distributed over the whole exposed metal surface. It refers to the corrosion that starts to move around the same rate all over the disclosed surface of metal. From the surface of metal regularly metal removal is known as uniform corrosion.

Ex:- Cast irons and steels corrode uniformly when exposed to open atmospheres, soils and natural waters, leading to the rusty appearance.



(a)



(b)

Fig:-2.1, Uniform Corrosion

In the above diagram (a) Steel plate is corroded uniformly over its entire surface. (b) The rusting of a pair of steel nuts used to fasten a galvanized steel clamp on a street lamp post.

2.2.2 Galvanic Corrosion

Galvanic corrosion is an electrochemical process in which one metal corrodes preferentially to another when both metals are in electrical contact, in the presence of an electrolyte. If two different alloys are joined in the presence of corrosive electrolyte. One of them will get corroded while the other is protected from corrosion. This corrosion may prevent through galvanic coupling. Stainless steel and Nickel may exist in either the passive or active state [27].

Ex:- Corrosion between welded carbon steel and stainless steel. Corrosion near the weld due to carbon steel pipe flange is active to the stainless steel.



Fig:-2.2, Galvanic Corrosion

The characteristic of galvanic corrosion is the corrosion near the junction between dissimilar alloy. Due to higher resistance corrosion decreases at points further from the junction through a longer electrolyte path.

2.2.3 Crevice Corrosion

When another material comes in contact the crevice is created. The localized attack on a metal surface at, or adjacent to, the gap or crevice between two joining surfaces. The gap or crevice can be formed between two metals or a metal and non-metallic material. The another material may be part of a fastener (bolt, rivet, washer) of the same or a different alloy, a deposit of mud, sand or other insoluble solid or a non-metallic gasket or packing.



Fig:- 2.3, Crevice Corrosion

Deposit and gasket corrosion terms are used when non-metallic material forms a crevice on the metal surface. If the crevice is made up of differing alloys or if the deposit is conductive (e.g. magnitude or graphite), crevice corrosion may be compounded by galvanic effects. Crevice corrosion of stainless steel in aerated salt solutions is widely.

Ex:- Stainless steel in hot salt solution.

2.2.4 Pitting Corrosion

Localized formation of small pits, generally that can't be simply seen by naked eye as they are easily hidden by inoffensive corrosion products surrounding its periphery. Sometimes pit may be deep shallow or undercut. Through which holes or cavities are generated in the material in localized form is known as pitting corrosion. Due to detection difficulties the pitting corrosion

is more dangerous than the uniform corrosion. The whole engineering system may be fail due to very small or narrow pit with very little loss.

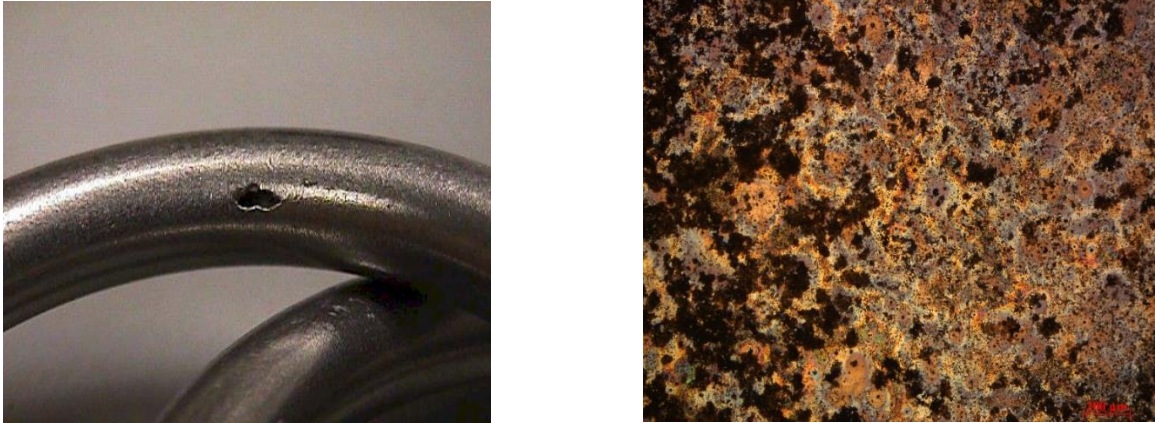


Fig:-2.4, Pitting Corrosion

2.2.4 Intergranular corrosion

The attack in the surrounding of the grain boundaries of the stainless steel is known as intergranular corrosion. Chromium carbides in the grain boundaries enter the very fast, due to this chromium depletion is there. The stainless steel is sensitized in some temperature range 540 to 860°C, so chromium carbides may be precipitated easily, as during welding or heat treatment such type of process occur[4].



Figure2.5:- Intergranular Corrosion

In the critical range if temperature lies for a long time, the formation of grain boundaries start due to chromium carbides, which then become capable to intergranular corrosion. Surrounding to the grain boundaries area becomes wasted in chromium (carbides formation is there due to

the reaction of chromium with carbon) and this area become less capable to resist the intergranular corrosion.

2.2.6 Hydrogen damage

Hydrogen damage is a general term which refers to mechanical damage of a metal caused by presence of or interaction by hydrogen. Hydrogen induced cracking generally predominates over stress corrosion cracking in carbon and low alloy steels, stainless steel, titanium alloys and aluminium alloys which have been alloyed, heat treated or cold worked to near maximum strength. The losses of fatigue life is contributed by Hydrogen induced cracking in such high strength alloys. Due to the atomic form of hydrogen the hydrogen damage is produced. The involvement of the reduced hydrogen ions is the production of hydrogen atoms and the subsequent formation of hydrogen molecules.



Fig 2.6, Hydrogen Cracking

In steel the hydrogen reacts with carbides and methane formation is there, resulting in surface blisters, voids and decarburization.

2.2.7 Erosion Corrosion and Fretting

Erosion corrosion comes due to the turbulent flow of fluid and corrosive fluid. Slow flowing fluid is the reason of low or modest corrosion rate, while the physically erosion occur by rapid transfer of the corrosive fluid and extracts the preventive corrosive layer, exposes the reactive alloy beneath and increase the degradation of the metal [5].

Due to the mechanical action, impinging fluid, abrasion by a slurry, bubbles or droplets, cavitation the degradation of the material surface is known as erosion corrosion.

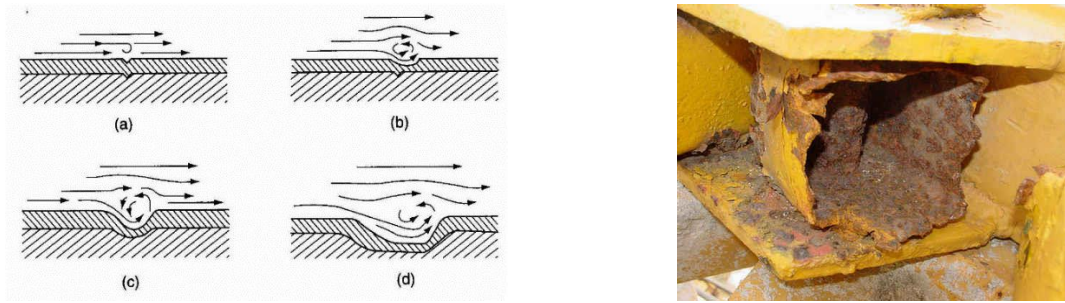


Fig:- 2.7, Erosion corrosion

In turbulent flow energy is released in the collapse of bubbles generation is cavitation. Erosion corrosion occurs due to energy transfer through water flowing over the surface of metal at speed more than 3 m/s wearing grooves in the metal by mechanical / chemical joint action. The effect of erosion corrosion has been seen on aluminium alloy frame of high-speed vessels.

2.3 Steel

Steel is an alloy of iron and another elements, mainly carbon, mostly used in manufacturing and other elements, due to high tensile strength and low cost, which is having the carbon percentage less than 2.1% and manganese is 1%. In other words we can say the steel is an interstitial solid solution of carbon in iron and having the carbon percentage less than 2.1%. The grade of steel is changed because of the changing the percentage of alloying element.

Stainless steel is the materials which is used for construction and manufacturing and having high corrosive-resistance, strength and fabrication property[6]. The proper stainless steel grades select on the basis of following qualities:-

1. **Corrosion or Heat Resistance**, the main reason for showing stainless. The specifier needs to know the surrounding condition and the chemical behavior or heat resistance needed.
2. **Mechanical Properties**, particularly strength at room, high or low temperature. The combination of corrosion resistance and strength is the basis for selection.
3. **Fabrication Operations** and how the product will be made (e.g., forging, machining, forming, welding, stamping, roll forming, four-slide operations).

4. **Total Cost**, including material and production costs and considering the cumulative savings of a maintenance-free product with longevity.

The corrosion, heat resistance and mechanical properties are all affected by the chemical composition of the stainless steel. As 304 and 316 steel grade as following:-

2.3.1 304 Stainless steel

This steel is highly resistive from corrosion. It resists decay of metal from oxidizing acid. This 304 SS is used for kitchen and food applications. However it is capable to corrosion from chloride solutions. Localized areas of corrosion can be created by chloride ions called as pitting, which can developed underneath protective chromium barriers to compromise internal structures.

304 SS is one of the form of stainless steel which is generally used in the surroundings. The composition of 304 stainless steel as follows:-

Element→	Ni	Cr	N	Fe	Si	Mn	C	P	S
Steel Grade↓									
304(Max%)	(8.00-12.00)	(18.00-20.00)	0.10	Balance	0.75	2.00	0.08	0.045	0.030
304L(Max%)	(8.00-12.00)	(8.00-20.00)	0.10	Balance	0.75	2.00	0.03	0.045	0.03

Table 2.1:- Composition of 304 stainless steel

This steel explained on the basis of different properties[7] as following:-

2.3.1.1 Corrosion and oxidation resistance

This 304 steel having highly corrosive resistance property to a wide range of environment, chemical, cloth and food industry exposure. 304 and 304L steel can be exposed up to 899 °C without scaling. For intermittent exposure, the maximum exposure temperature about 815 °C.

2.3.1.2 Heat treatment and formability

Type 304 steel can not be harden by heat treatment process. For annealing the heat require from 1038 to 1130 °C. Thin strip can be cooled by air but for heavy sections the water

quenching is necessary for minimize exposure in the carbide precipitation area. This steel have good drawability. Due to the low yield strength and high elongation it permits very easily to form complex shape. After forming the parts should be full annealed or stress relief annealed to relieve stresses produced in severe forming or spinning.

2.3.1.3 Weldability

By the common fusion and resistance technique this type of steel is considered to be good weldable. AWS E/ER 308, 308 L, 347 are mostly specified, when the weld filler material is needed.

2.3.1.4 Physical and mechanical properties of 304 stainless steel

Property	Minimum Value (S.I.)	Maximum Value (S.I.)	Units (S.I.)	Minimum Value (Imp.)	Maximum Value (Imp.)	Units (Imp.)
Atomic Volume (average)	0.0069	0.0072	m ³ /kmol	421.064	439.371	in ³ /kmol
Density	7.85	8.06	Mg/m ³	490.06	503.17	lb/ft ³
Energy Content	89	108	MJ/kg	9642.14	11700.6	kcal/lb
Bulk Modulus	134	151	G-Pa	19.435	21.9007	10 ⁶ psi
Compressive Strength	205	310	MPa	29.7327	44.9617	ksi
Ductility	0.3	0.57		0.3	0.57	NULL
Elastic Limit	205	310	MPa	29.7327	44.9617	ksi
Endurance Limit	175	260	MPa	25.3816	37.7098	ksi

Fracture Toughness	119	228	MPa.m ^{1/2}	108.296	207.491	ksi.in ^{1/2}
Hardness	1700	2100	MPa	246.564	304.579	ksi
Modulus of Rupture	205	310	MPa	29.7327	44.9617	ksi
Poisson's Ratio	0.265	0.275		0.265	0.275	NULL
Tensile Strength	510	620	MPa	73.9692	89.9234	ksi
Young's Modulus	190	203	G-Pa	27.5572	29.4426	10 ⁶ psi
Maximum Service Temperature	1023	1198	K	1381.73	1696.73	°F
Melting Point	1673	1723	K	2551.73	2641.73	°F
Specific Heat	490	530	J/kg-K	0.37919	0.41015	BTU/lb.F
Thermal Conductivity	14	17	W/m-K	26.2085	31.8246	BTU.ft/h.ft ² . F
Thermal Expansion	16	18	10 ⁻⁶ /K	28.8	32.4	10 ⁻⁶ /°F

Table 2.2:- Properties of 304 Stainless steel

2.3.2 316 stainless steel

316 steel is the another form of stainless steel. Approximately the properties are same as 304 stainless steel. Which makes the different of 316 stainless steel as compare to 304 stainless

steel i.e. percentage of molybdenum, by adding molybdenum the corrosion resistance of the steel increases- specially against chloride and some other solvent which are used in industries. Generally 300- series steel grades having up to 7 percent molybdenum.

The composition of other alloying element are as follows:-

Element→	Ni	Cr	Mo	Fe	Si	Mn	C	P	S
Steel Grade↓									
316(Max%)	12.00	17.00	2.50	Balance	0.75	2.00	0.08	0.045	0.03
316L(Max%)	10.00- 14.00	16.00- 18.00	2.00- 3.00	Balance	0.75	2.00	0.03	0.045	0.03

Table 2.3:- Composition of 316 Stainless steel

This steel explained on the basis of different properties as following:-

2.3.2.1 Corrosion resistance

316 stainless steel having better corrosion resistance than type 304. This type of steel gives good pitting resistance and excellent resistance to most chemicals involved in the paper, clothes and photographic industries.

2.3.2.2 Weldability

Due to the common fusion and resistance technique this type of steel is considered to be good weldable. AWS E/ER 308, 308L, 347 are mostly specified, when the weld filler material is needed. 316 and 316L stainless steel having poorer weldability than 304 and 304L. Due to the higher nickel percentage for these alloys needs the slower arc welding speed and more care to avoid hot cracking. AWS E/ER 316L and 16-8-2 are specified, when a weld filler material is required.

2.4 Pitting Corrosion

Pitting corrosion is the generalized initiation of small pits that can't be seen simply through naked eyes as they are easily hidden by inoffensive corrosion products surrounding its periphery, results in relatively rapid penetration. This is unpredictable type of corrosion and pretentious and hence it can give result as destruction of meatal. The stainless steel which used

in marine and chemical industries are seen to have pitting corrosion. The pitting occurs generally in presence of chloride ions. The pitting corrosion penetrates the metal mass, with limited diffusion[8,9].

2.4.1 Mechanism of pitting corrosion

This type of corrosion is generally catalytic in environment. When the process has been started, it has the capability to maintain the nature conditions. Pitting occurs due to passivity breakdown at very small isolated sites distributed at the metal surface and generate local active/passive cells. Due to heterogeneities in the surface of metal pitting formation can be initiated because of minority phases in the microstructure of metal[9].

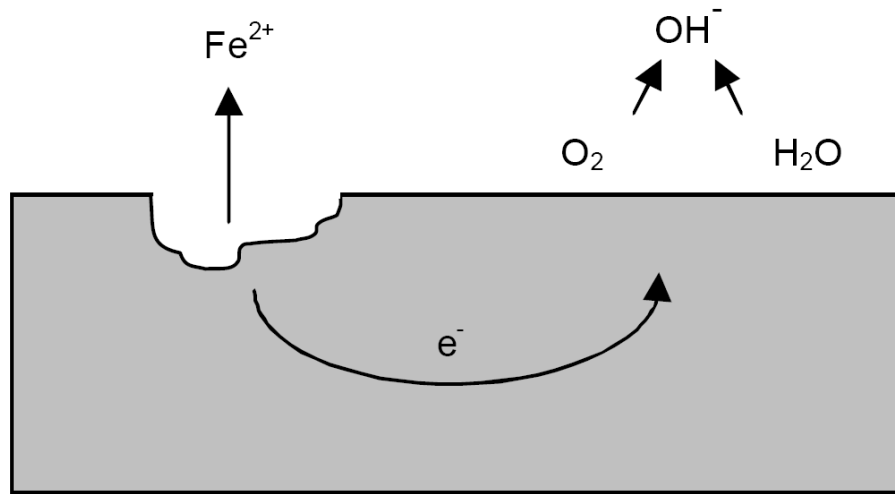


Fig 2.8:- Mechanism of localized corrosion developing on metal in a solution containing oxygen

This kind of corrosion is extremely dangerous, due to this material losses occur with less effect on the metal surface, as it damages the more surface of metal. The pits on the surface are often obscured by corrosion products[10]. Pits formation can be started due to a small surface defect, being a little change in composition or layer which form due to passivity may be destroy. In the sodium chloride solution the metal pitting M is showing in the figure 2.9.

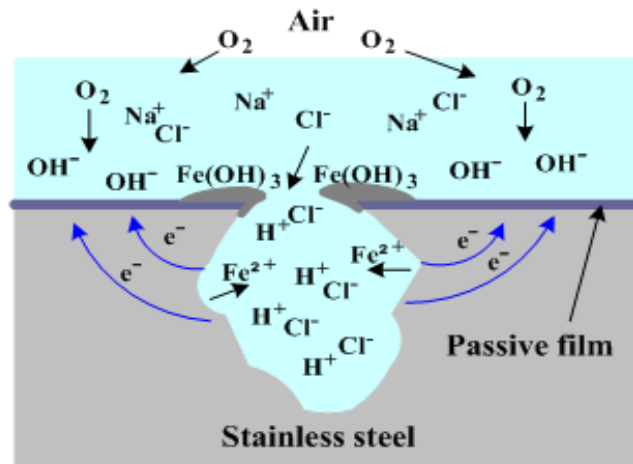


Fig 2.9:- Corrosion mechanism

While the cavity is anodic from inside, the outer surface around to the cavity work as cathode. The cavity or pit is charged as positively from inside, due to quick dissolution of the metals, the chloride ions which are negatively charged are attracted to the pit for supporting electro neutrality. To form MCl inside the pit this negatively charged chloride ion (Cl^-) reacts with the metal, due to that the pH is decreased, more and more metal dissolution is highly simulating. A safe and preserved area are provide by the pit which prevents easily mass transport between external bulk solution and pit. The oxygen solubility is very less in concentrated solution, and inside the pit there is no oxygen reduction[11]. Pitting formation start when the potential comes more than the critical pitting potential, E_{pit} , to measure the resistance pitting corrosion E_{pit} is used. Higher value of the pitting corrosion gives the significance of more resistance to pitting corrosion and lower the value of E_{pit} shows the lesser resistance to pitting corrosion. Anodic current increases due to presence of chloride ions at all higher potentials as shown in figure. But here due to presence of chloride ion the value of pitting potential (E_{pit}). Above E_{pit} the current increases drastically, it shows the breaking of the protective film on the metal surface.

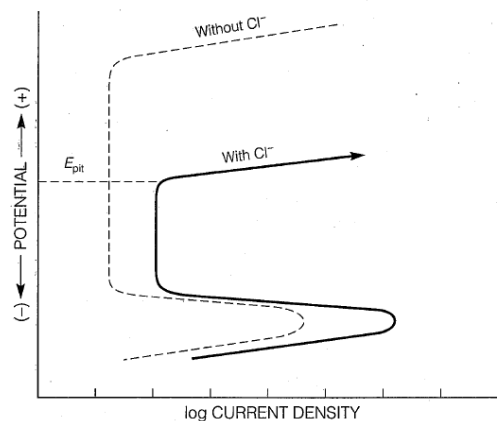


Fig 2.10:- Formation of pitting above E_{pit}

When the film breaks and corrosion products give the effective mass transfer and between the bulk solution and underlying metal and there is no chemical reaction takes place. On the tip of the pit the deposition was formed by the corrosion products and inside the pit helps to accelerate the rate of dissolution prevents the flow of mass . When the pit formation is there, the pit can grow continuously inside the cavity to form a discontinuity. The established condition is necessary for developed pit. If required conditions are not reached the pits growth will stop. The pitting corrosion depends on the alloy composition, to find this condition the various parameters are there which tells about the condition of pitting corrosion on alloy based. Figure 2.10 shows the initiation, formation & pits expansion on the metal (iron) by the external protective passive layer[9,26].

The accumulation of the localized corrosion damage (LCD) are breakdown of passivity and formation of pits, which occur in highly corrosive environment having concentrated chloride. Subsequently, the pits that grows to critical dimensions act as sites for the cracks nucleation. Therefore, breakdown of passivity and nucleation of pits on the 304 stainless steel having more importance in relevance to the risk associated with the operation of different major industries which fulfill the basic needs of our substance. A deterministic description of passivity breakdown on metal and alloys is provided by the point defect model (PDM). Past characterization of passivity was working on the analytical observation but with the growing

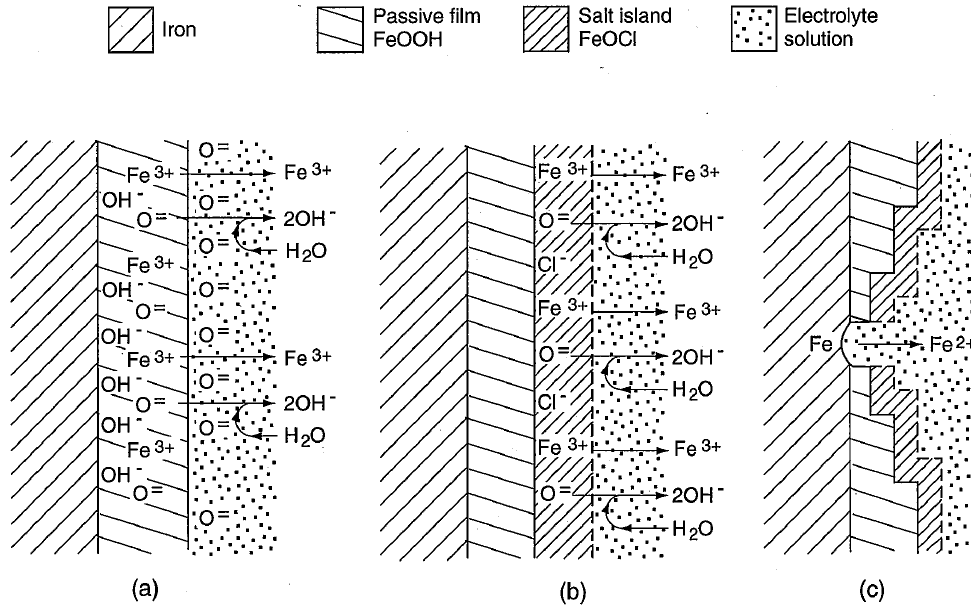


Fig 2.11:- Pitting on iron (a) Initiation due to the passive film dissolution, (b) At a soluble salt island accelerate dissolution, (c) Pit formation due to direct anodic dissolution

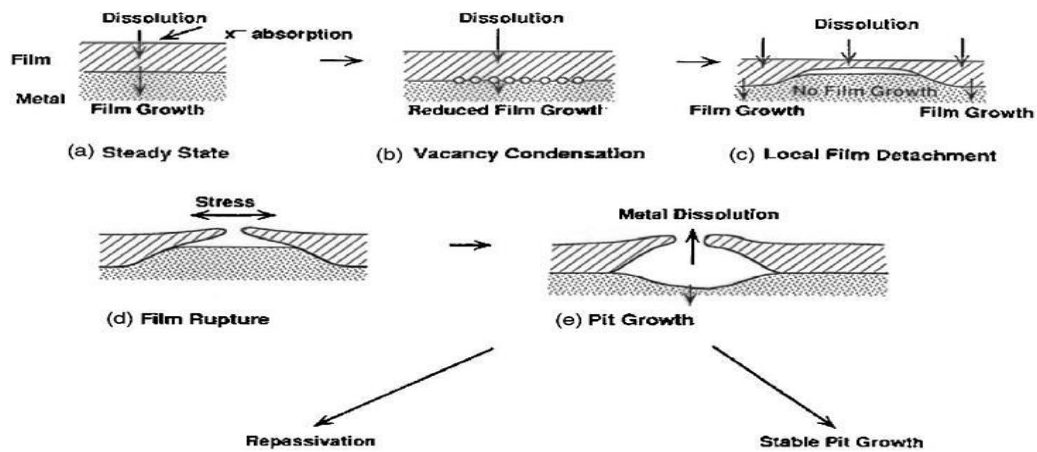


Fig 2.12:-Pitting corrosion stages

of modelistic approach, the passivity characterization and stability and breakdown of passivity can be evaluated, following are the comparison between the two can be made and the validity of the model can be estimated.

2.5 Initiation and growth

The surface of the metal is protected by the formation of a 3 dimensional oxide layer i.e. passivity. Hence the discovery of passivity, various laws and equations were described to account for the development of the passive layer, and finally, the growth kinetics was attributed to the following laws where experimentally data shows both having equal credibility[13,14].

$$L = A + B \ln t \quad (\text{logarithmic law})$$

$$1/L = C - D \ln t \quad (\text{Inverse logarithmic law})$$

Where, $A, B, C, D = \text{constant}$

$L = \text{film thickness}$

$t = \text{time}$

For experimental analysis, various models were discovered to follow the above laws. Some of those models are as follows [25]:-

- (a) Mott – Cabrera Model
- (b) Sato and Cohen's Model
- (c) Fehlnner and Mott's Model
- (d) Point Defect Model (PDM)

For our analysis we will use 'Point Defect Model (PDM)'. Point defect model has been discussed as follows:-

2.5.1 Point Defect Model (PDM)

Three generations of point defect model have been developed, with each evolving to address critical issues of the previous generation that became apparent upon comparison with experimental data. The assumption of three generations of the PDM is defined as[15]:-

Generation 1:- PDM-1 imagined that the passive film included a single defective oxide layer that impeded the current flow across the metal/ solution medium. Assumption of the PDM-1 generation given as:-

- Due to the formation of oxide layer the point defect phase having oxygen and cation vacancies.
- The point defect concentration is greater than in the isolated, bulk oxides, the defect generation (and annihilation) process is the indication of the point defect.
- The generation and annihilation defects occur on the metal/ film (m/f) and film/ solution (f/s) region.
- The electric field strength (ϵ) is independent of voltage and distance through the film. The former is due to band to band tunneling, such that as the field strength tends toward a higher value the bands become steeper and the tunneling distance for electrons from the valence band to the conduction band (or to inter band gap states) decreases, thereby resulting in higher tunneling current. This produces a separation of charge that opposes the field and essentially buffers the field at an upper, voltage independent value of 2-5 MV/cm.
- The electrostatic potential is distributed across the interphase with drops across the m/f interface, the film/ solution interface and the film, where L is the thickness of the film.

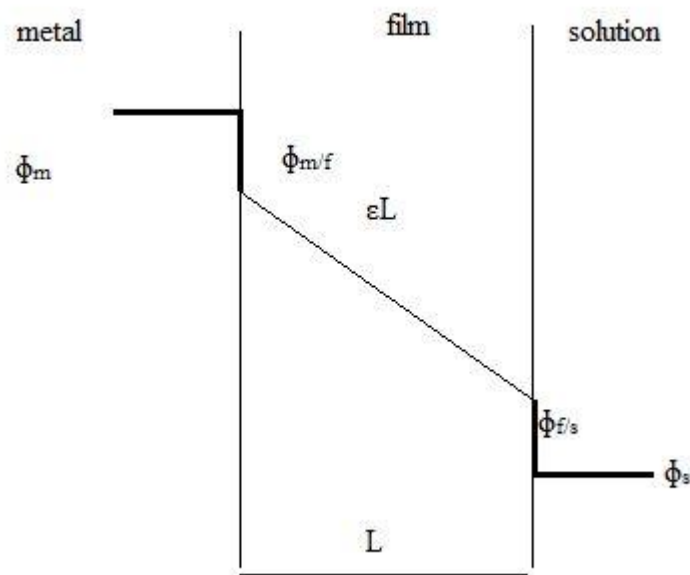


Figure 2.13:- Potential distribution across the metal/ barrier layer / solution interface

- The voltage drop over the film/ solution interface is linearly dependent on the applied voltage and the pH i.e.

$$\phi_{f/s} = \alpha V + \beta \cdot \text{pH} + \phi_{f/s}^{\circ} \quad (1.)$$

where, α = polarizability of the film / solution interface

β = dependence of the voltage drop over the f / s interface on pH

$\phi_{f/s}^{\circ}$ = value of $\phi_{f/s}$ when $V = 0$ and $\text{pH} = 0$

Generation- II:- The generation-II point defect model came to overcome the problems in generation-1 model. The assumptions of the generation-II model as follows:-

- Recognizes the role played by barrier layer dissolution – allows the film to achieve steady state in thickness and current. The barrier layer dissolves at the barrier layer / solution (outer layer) interface by either chemical or electrochemical process.
- Recognizes and classifies interfacial reactions as to whether they are lattice conservative or non-conservative process.
- Introduces interstitials in addition to cation vacancies and oxygen vacancies as the defects in the barrier layer.

Generation- III:- The assumption for the generation-III model as following:-

- The model must incorporate the outer layer in the passive film as an active electrochemical element. By ‘active’ is meant that the outer layer participates in determining the potential differences across the film and hence in determining the passive current density.
- The IR potential drop subtracts from the applied potential in determining the potential that exists at the barrier layer / outer layer interface and hence determines the fraction of the applied potential that drives the growth of the barrier layer.
- Because of the IR potential drop across the outer layer, the outer layer has a profound effect on the properties of the barrier layer.

- If the outer layer resistance is sufficiently large, it may dominate the interfacial impedance and hence determine
- If the IR potential drop is sufficiently large, the barrier layer may disappear corresponding to ‘resistive depassivation’ but not necessarily in loss of corrosion resistance (because of the existence of the resistive outer layer).

2.6 Passivity

Passive film thickness should be as much as possible for the study of generation and stability of the passive film. As the passive film is a semiconductor device, film nature, it is p- type or n- type, also plays important role. Many techniques are there which may give information about the thickness and nature of the film as electrical chemical impedance spectroscopy and mott schottky analysis [21]. Anionic vacancies and interstitials gives the result as n-type passive films formation but p-type films form by the cationic vacancies movement. The behavior of the films depend on the external potential, film can behave either n-type or p-type. The point defect proved by the development of film that can follow as logarithmic and inverse logarithmic law. According to the point defect model, the growth of film occurs due to diffusion of anionic vacancies while metal dissolution due to cation vacancies[16]. The reactions occur at the metal / film and film / solution interface as shown in figure. When PDM was compared with the potentiodynamic curve data, there was various errors find, finally PDM-1 was failed.

PDM-1 was failed because of [15]:-

- Generation-1 PDM was not valid for steady states in passive current density & barrier layer thickness.
- The barrier layer may became apparent, mobile donor must be there, if the film is n-type other than the oxygen vacancy that can account for the current. That species was subsequently identified as the cation interstitial.
- PDM-1 did not compare b/w the reactions as to their lattice conservation & it did not recognize the formation of the outer layer. Due to the failure of PDM-1, then in 1990s PDM-II came.

The thickness of the film (L_{ss}) is dependent on the applied potential. From the anodic polarization curve the thickness of the film increases with the anodic polarization in the positive direction. The value of I_{ss} does not depend on the applied potential. Many experiments has been done which include PDM to represent for the passivity [15].

$$L_{ss} = \frac{1}{\varepsilon} \left[1 - \alpha - \frac{\alpha \alpha_7}{\alpha_3} \left(\frac{\delta}{x} - 1 \right) \right] V + \frac{1}{\varepsilon} \left\{ -\frac{2.303n}{\alpha_3 x \gamma} - \beta \left[\frac{\alpha_7}{\alpha_3} \left(\frac{\delta}{x} - 1 \right) + 1 \right] \right\} pH + \frac{1}{\alpha_3 x K} \ln \left(\frac{k_3^0}{k_7^0} \right) \quad (2)$$

$$I_{ss} = \delta F [k_2^0 e^{a_{2V}} e^{b_{2L_{ss}}} e^{c_{2pH}} + k_4^0 e^{a_{4V}} e^{c_{4pH}} + k_7^0 e^{a_{7V}} e^{c_{7pH}} \cdot \left(\frac{C_{H^+}^0}{C_{H^+}} \right)^n] \quad (3)$$

Where, L_{ss} = Film thickness

I_{ss} = Passivation current density

δ and x = metal cation oxidation states in the barrier layer and in the solution (outer layer).

ε = Relative permeability of the passive film

α = Polarizability

α_s = Diffusion factor where s is the equation number in Generation II model

k_s = Rate constant of the equation

n = Number of electrons

2.7 Passivity breakdown

Cation vacancies ($V_M^{x'}$) generated at the film / solution interface move to the metal / film interface is proposed by point defect model i.e. shown in figure, and are destroyed by cation injection into the film from the metal[15,17].



Where, m and v_m = In the metal phase metal atom and metal vacancy

$V_M^{x'}$ and M_m = On the cation sub lattice of the barrier layer cation vacancy and a cation in normal cation sites.

The annihilation rate of the cation vacancies at the m/f interface is shown as J_m . Into surface oxygen vacancies (V_o'') aggressive anion (chloride anion) absorption catalyzes the cation vacancies generation through a schottky pair reaction and cation vacancies (J_{ca}) flux increased toward the m/f interface. If J_{ca} greater than J_m , the cation vacancies condensate at the m/f interface, the barrier layer removes from the substrate metal, if the areal concentration in the condensate exceeds a critical value(ξ) [18]. This local separation process proceeds at the boundary of the condensate causing the condensate to extend and escaping the layer from penetrating into the substrate by producing of oxygen vacancies via,



However, at the outer surface there is dissolution continues with the result that the barrier layer over the condensate thins at a rate that is found by the dissolution rate and somewhere the ‘cap’ (remnants of the barrier layer) over the condensate will break to mark passivity breakdown event.

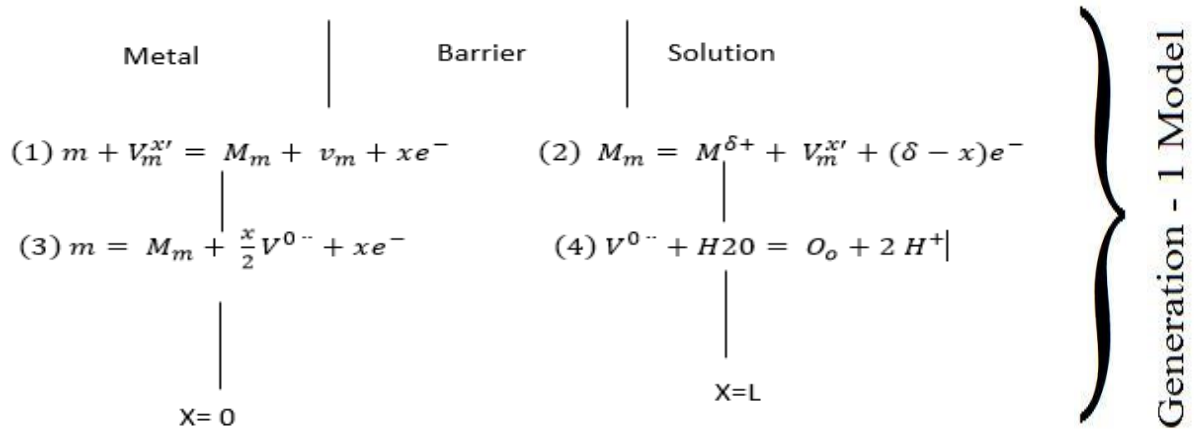


Fig 2.14:- Generation-1 Point defect model

Critical concentration of the cation vacancies that must condense per unit area (ξ) for separation to occur between the barrier layer and the metal substrate is determined through the metal

structures and the structures of film, depending on whether condensation is imagined to occur on the film that film may be of cation sub lattice or metal lattice. The reaction scheme gave in PDM-1 for the generation and annihilation of cation vacancies as shown in figure 13. The cation vacancies are generated at the film/ solution interfaces and it is consumed at the metal/ film interfaces. In this reaction scheme PDM-1, there is no medium for metal as point defects and no description about the dissolution of the barrier layer. Figure 2.14 gives the group of equations which are described by the PDM-1.

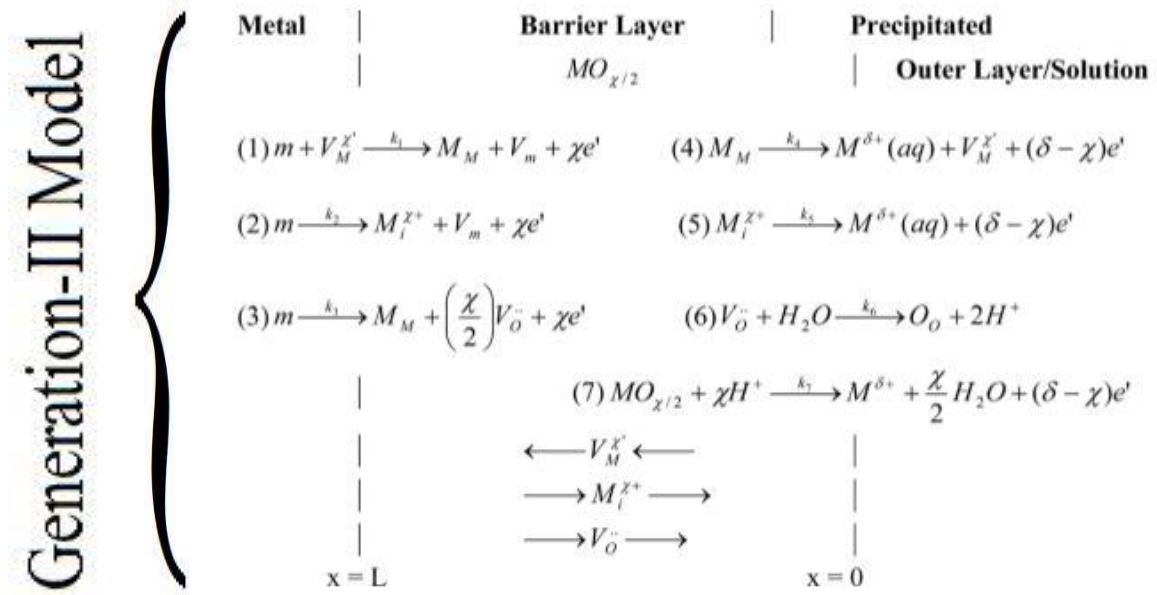


Fig 2.15:- Generation-II Point defect model

The critical breakdown potential (V_c) was derived, according to the above mechanism, chloride ion adsorption schottky-pair vacancy generation,

$$V_c = \frac{4.606RT}{x\alpha F} \log\left(\frac{b}{D}\right) - \frac{2.303RT}{\alpha F} \log(a_{Cl^-}) \quad (6)$$

$$\text{Where, } b = \frac{RTJ_m\Omega}{F\chi\epsilon N_v} \times \exp\left(\frac{\Delta G_s^0 + \frac{\chi}{2}\Delta G_A^0 - \frac{\chi}{2}\beta FpH - \frac{\chi}{2}F\phi_{f/s}^0}{RT}\right) \quad (7)$$

$$\phi_{f/s} = \phi_{f/s}^0 + \alpha V + \beta \cdot pH \quad (8)$$

As in the first generation give all observation, PDM-II was introduced with added some equations to represent the errors. From critical breakdown potential we can say, if chloride concentration increases then breakdown potential (V_c) decreases and vice versa. The value of the polarizability constant (α) can be find from the slope of the curve. The pH dependence may be find out from the equation. The breakdown potential increases with increasing pH and the slope of this curve gives the result value of β and film / solution interface potential depends on pH [15,19].

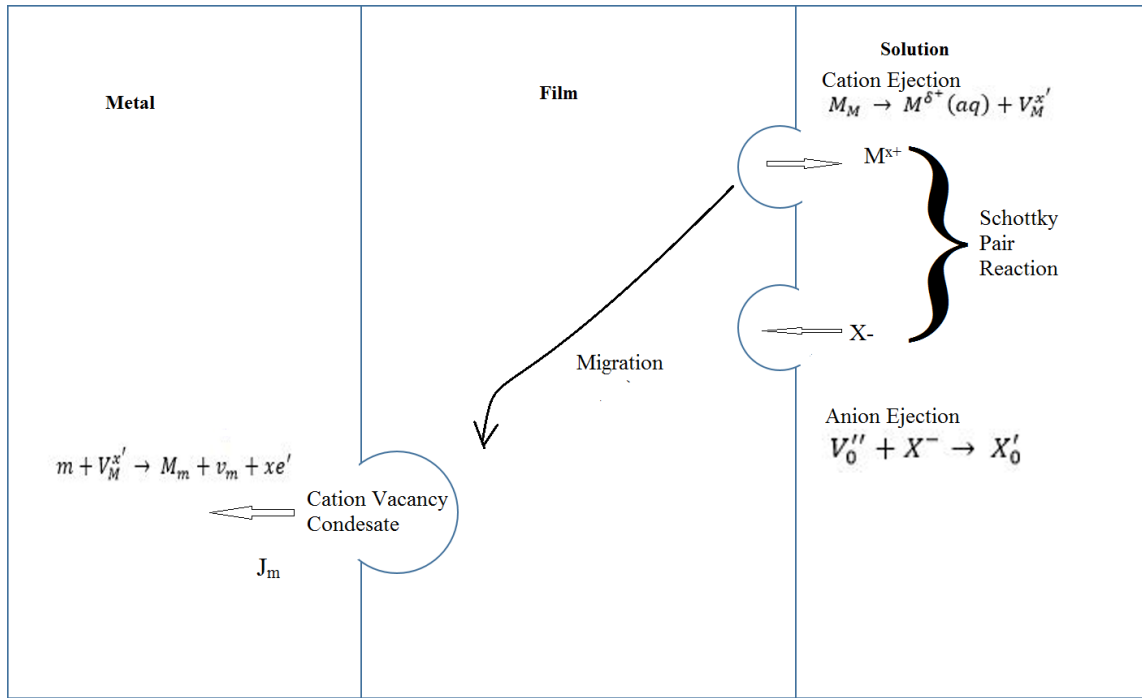


Fig 2.16:- The breakdown of passive films on the basis of PDM

Breakdown of passivity is imagined to occur at place on the metal surface, described through the high cation vacancy diffusivity. These sites are supposed to include highly entropic structure of the barrier layer that might exist, at intersection point of the barrier layer with inclusions. The breakdown voltage are supposed to be normally distributed compare with diffusivity of cation vacancy with the distribution characterized by a mean value \bar{D} , and the

standard deviation σ_D . an analytical distribution function for breakdown potential (V_c) is find out from the following equation.

$$\frac{dN}{dV_c} = \frac{-b\gamma'}{\sqrt{2\pi} \sigma_D a_{Cl^-}^{x/2}} \exp \left[\frac{-(e^{-\gamma' V_c} - e^{-\gamma' \bar{V}_c})^2 b^2}{2\sigma_D^2 a_{Cl^-}^x} \right] \exp(-\gamma' V_c) \quad (9)$$

Where,

$$\gamma' = \frac{x\alpha F}{2RT} \quad (10) \quad \bar{V}_c = \frac{1}{\gamma'} \ln \left(\frac{b}{D} \times a_{Cl^-}^{-x/2} \right) \quad (11)$$

In breakdown potential the cumulative probability is explained in following equation, percentage breakdown sites at breakdown potential (V_c) in all possible breakdown sites is $P(V_c)$.

$$P(V_c) = \frac{\int_{-\infty}^{V_c} \left(\frac{dN}{dV_c} \right) dV_c}{\int_{-\infty}^{\infty} \left(\frac{dN}{dV_c} \right) dV_c} \times 100 \quad (12)$$

2.8 Summary

Pitting corrosion is the form of corrosion that takes place with the chloride ions through breakdown of passivity. The passivity characterization has been addressed through different models. Phenomena of passivity and passivity breakdown is well explained by point defect model and development of film kinetics. Point defect model is the model which is clearly explained the passivity and breakdown of passivity with the experimental data.

Chapter 3

Materials & Methods

304 stainless steel polished samples were prepared and studies of passivity and its breakdown at different chloride $[Cl^-]$ ions concentration in borate buffer solution, varying pH and different potential sweep rate. The details and methods which were used for experiment to study the same along with the preparation of the solution has been explained in this chapter.

3.1 Sample preparation

The composition of 304 stainless steel is given in Table 2.1. Due to high percentage of chromium the 304 stainless steel having corrosion resistance property and work as austenite stabilizer in presence of nickel.

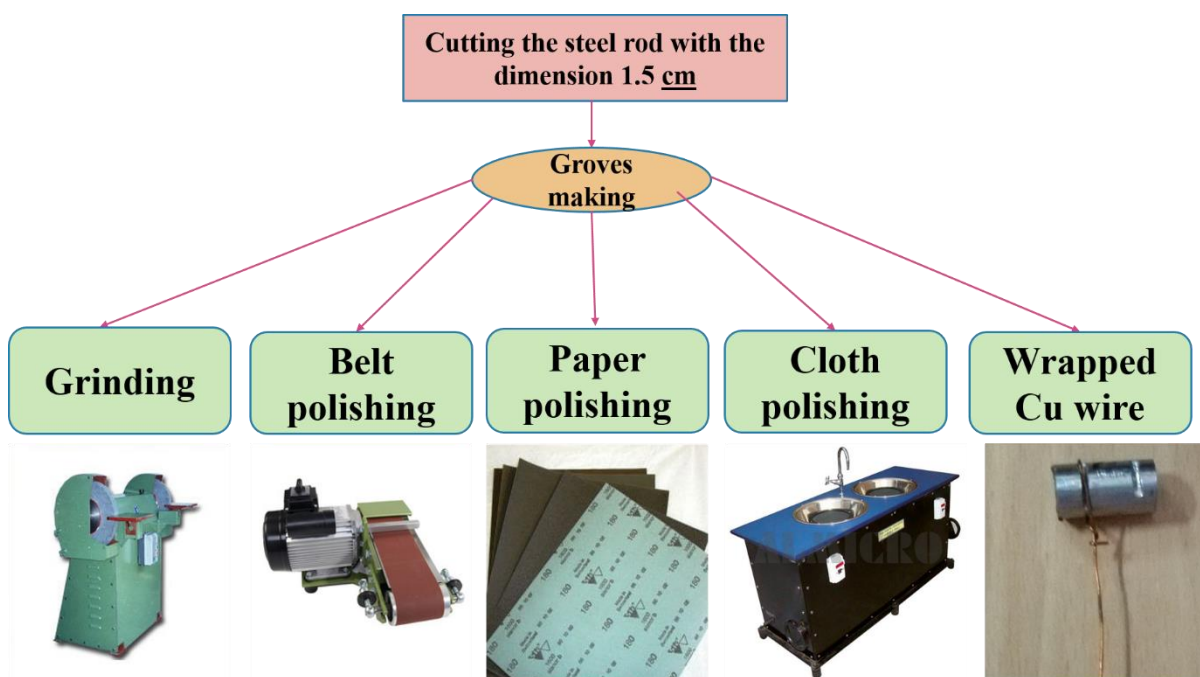


Fig. 3.1:- Steps used for sample preparation

3.1.1 Grinding and polishing

The 304 stainless steel specimens cut from round bar or rod that's diameter is around 0.8 cm. After cutting the samples were grinded on the metal grinder and then grooves were made for holding the samples with copper wire. And then polished by the belt polishing. The specimen with emery paper of grade 1/0, 2/0, 3/0, 4/0 for about 5 to 10 minutes on the emery paper and 90 degree rotated one by one paper. Then specimen polished on thick cloth through the alumina. Up to cloth polishing through alumina around 90% scratches has been removed. Finally the specimens were polished on the diamond polisher until looking like mirror image with close to zero or without scratch. This diamond polishing completed through diamond spray and diamond paste. Then the copper wire is wrapped in the groove to prepared final sample and the working surface area is 0.5 cm^2 . The steps of the sample preparation is shown in figure 3.1 [20].

3.2 Solution preparation

Here for our experiment we use borate buffer solution at different pH. A buffer solution (more precisely, pH buffer or hydrogen ion buffer) is an aquatic solution and having the mixture of a weak acid and its conjugate base, or vice versa [21]. If small or more percentage of acid or base is added it results small changes in pH.

Chances of localized changes is there in pH because of pitting corrosion, by using borate buffer that can be avoided. With different chloride concentration the borate buffer at varying pH were prepared for our study.

S.No.	pH	Boric Acid	Sodium Hydroxide
1	8.3	0.76 M, 47 gm	0.2 M, 8 gm
2	9.3	0.1 M, 6.183 gm	0.05 M, 2 gm
3	10.3	0.1M, 6.183 gm	0.1 M, 4 gm

Table 3.1:- Composition of buffer solution

Add water up to 1 L. To make the borate buffer solution the boric acid and sodium hydroxide pallets were used. After adding the chloride the pH was changed. To maintain the pH again 1M NaOH was added drop by drop through pipet. Here the chloride concentration was added at different concentration as 0.1M, 0.5M, 1M at different pH. In table 3.1 the composition of borate buffer solution is showing.

3.3 Electrochemical Setup

Potentiodynamic polarization is a method where the electrode potential is changed at a selected rate by applying a current through the electrolyte. All experiments were conducted in a single comparted glass cell by using a 'Gamry Potentiostat'. Generally the potentiodynamic polarization method is used for the corrosion studies. Diagram of electrochemical cell is shown in figure 3.2. The 304 stainless steel specimen after joined the copper wire dipped into the electrolyte as shown in figure. The graphite rod was used as a counter electrode i.e. sealed in a glass that was fitted in another glass tube [22]. The reference electrode was saturated calomel electrode that was fitted in a Luggin capillary with a cracked glass tip. The polished surface of stainless steel was worked as a working electrode. All experiments done at room temperature.

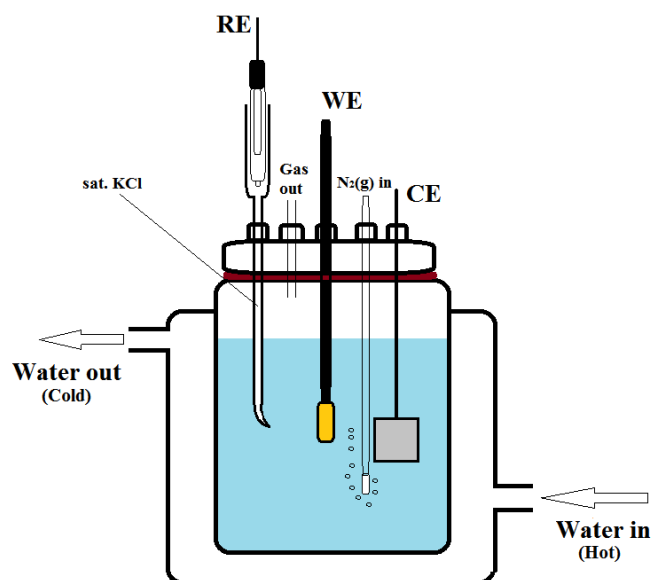


Figure 3.2:- Three electrode electrochemical setup

After getting the data from potentiostat, the D.C. source used for further studies. In D.C. source we have to use 2 electrode system as cathode and anode [22]. On the same condition of pH and chloride concentration buffer solution is used. We have taken 4 voltage in passive region and run on those potential, then run those samples on breakdown potential which determined from the potentiodynamic curve.

3.5 Optical microscope

In the Optical microscope the visible light is used and lens system uses for magnify images of small images. Optical microscope is used for seeing the microstructure of the materials at different magnification (5X, 10X, 20X etc.) [23]. After completing the work in D.C. source, the microstructure was seen in optical microscope for seeing the condition of pitting by microstructure.

3.6 Electrochemical Measurements

Different plots of potentiodynamic were plotted to get the different types of values to represent for the modelling part in PDM. The study of passivity is done by plotting the potentiodynamic curves and selected the four voltages at which the passive layer was generated on the metal and to find the defect another analysis was used i.e. Mott Schottky analysis [24], it may be p-type or n-type. From PDM the calculation were done for L_{SS} and I_{SS} .

At various chloride concentration a_{Cl^-} (0.1M, 0.5M, 1M) and at various pH the potential verses current plots were plotted. From this data a curve drawn between cumulative probability and breakdown potential. The various scan rate were used as 0.167, 1, 5, 10, 50, 100 mV/seconds. Around 10 to 20 times the potentiodynamic curve plotted for determine the cumulative probability distribution of breakdown potential at various pH and chloride concentration. At different pH the potentiodynamic plots were also used to find the value of β .

Chapter 4

Results and Discussions

This chapter precise different curves of potentiodynamic i.e. determined from the experimental data, and helps to derive the some parameter which defined in Point Defect Model for the analysis of passivity breakdown through computational modelling. The superimposed the modelling curve with the experimental data.

4.1 Passivity studies of 304 stainless steel

The curve plotted of the potentiodynamic at the scan rate of 0.167 mV/s, to determine the cathodic and anodic polarization data as shown in figure 4.1. From E_1 to E_4 passive region is showing. Four potentials we have taken for analyze the passive film on this grade of steel [27].

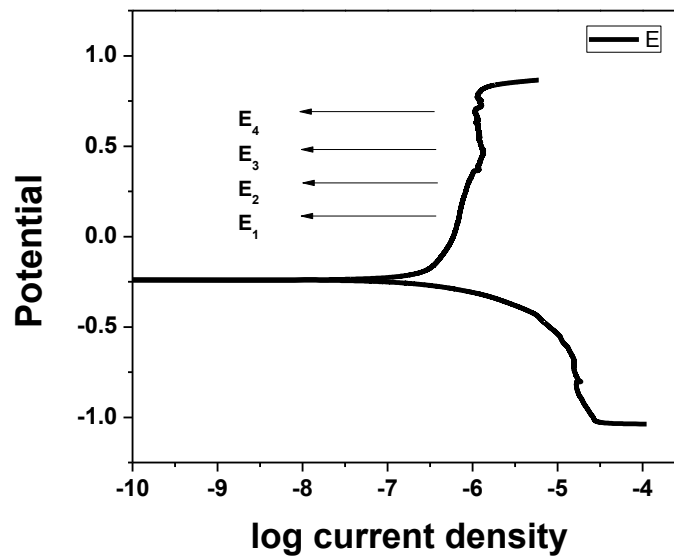


Fig 4.1:- The curve for potentiodynamic polarization of 304 SS in buffer solution

The solution is prepared having a pH is 9.3 with no chloride concentration. Open Circuit Potential (OCP) for four samples is showing in figure 4.2 [15].

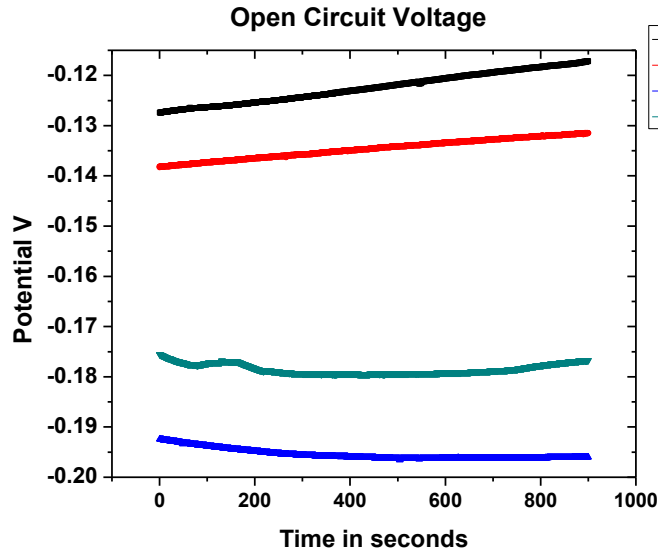


Fig 4.2:- Open circuit voltage for 304 SS in borate buffer solution

Around 900 seconds the OCP was run. The OCP was used for stabilizing the sample, without stabilize it does not give good result. The OCP played a very important role in this experiment that the metal with low open potential will dissolve quickly in the solution than the metal with high OCP.

4.2 Breakdown potential for 304 stainless steel at room temperature

The breakdown potential of 304 stainless steel is based on the concentration of chloride, breakdown potential decreases, if chloride concentration is increasing. Figure 4.3 is showing a potentiodynamic plots at a scan rate of 1 mV/s with different chloride concentration and without chloride containing deaerated buffer solution. As the potential goes into the positive direction, there is slow increase the current density until getting the passivation area, where the passivation region obtains, the current density goes to approximately constant, where drastically the current density is increased that is known as characteristic of breakdown of passivity and where the breakdown of passivity lies that potential is known as breakdown potential[28].

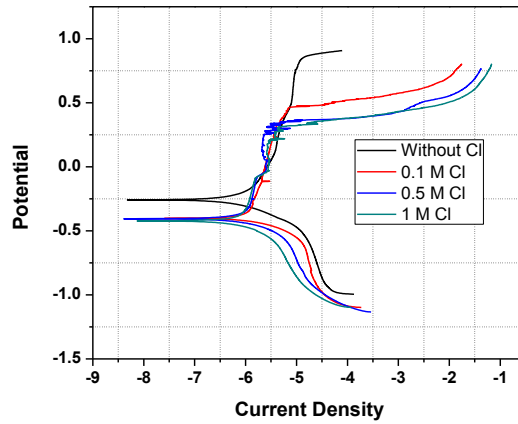


Fig 4.3:- Curves for potentiodynamic polarization 304 stainless steel in varying chloride concentration containing buffer solution at pH=9.3 at room temperature (scan rate=1 mV/s)

As chloride concentration increases, the breakdown potential decreases. And the breakdown potential decreases linearly with chloride ion activity as shown in figure 4.4

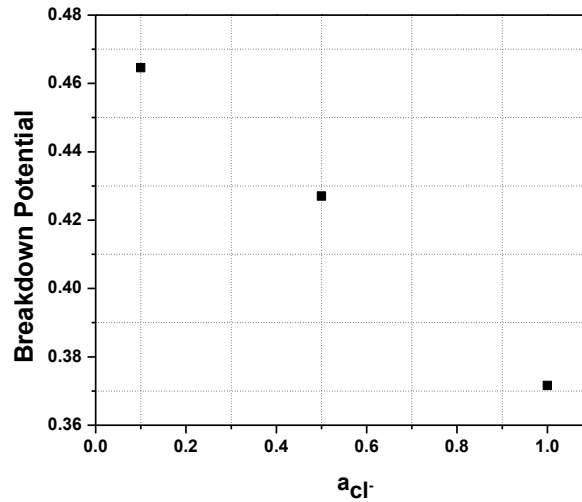


Fig 4.4:- Breakdown potential at scan rate= 1mV/s for 304 SS in borate buffer solution having pH=9.3 is a function of the chloride ion activity

By using the Eq No. 6 and from figure 4.4 the slope determined, the value of α can be determined, slope of the curve = $-\frac{2.303RT}{\alpha F}$

Where, R= Universal gas constant

T= Temperature

F= Faraday's constant

According to the PDM the breakdown potential (V_c) depends on the scan rate(v) of the potential through the following equation:-

$$V_c = \left(\frac{2\xi RT}{J_m \alpha F} \right)^{\frac{1}{2}} v^{\frac{1}{2}} + V_c(v = 0) \quad (13)$$

Where, ξ is represent to the areal concentration. The separation of the barrier layer from the substrate metal is the reason of condensed cation vacancies at the metal / barrier layer interface, due to this the breakdown of passivity occur and J_m is the annihilation rate of cation vacancies that goes into the metal phase at the boundary of condensate cation vacancy [29,30].

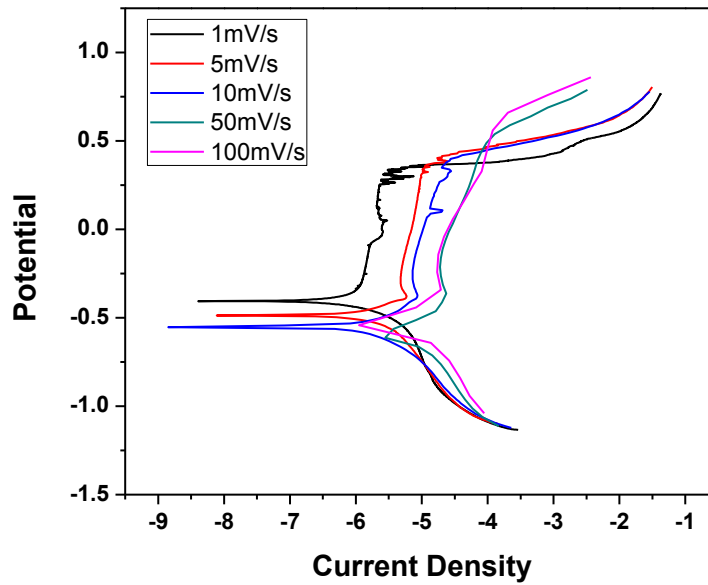


Figure 4.5:- Polarization curve shows the dependency of breakdown potential on scan rate

At zero potential scan rate the breakdown potential is represented by $V_c(v=0)$. α is the polarizability of the barrier layer to solution. The polarization curve at different potential scan

rate is showing in figure 4.5. This figure shows if the potential scan rate increases then the breakdown of potential also increases and with the increasing potential scan rate the current at breakdown potential increases.

4.2.1 Distribution of breakdown potential and its calculation

The PDM is used to predict the formulation for obtaining the breakdown potential distribution which follows a normal distribution of potential breakdown sites in comparison to cation vacancy diffusivity (D) characterized by a mean value of \bar{D} (the mean cation vacancy diffusivity) and a standard deviation σ_D (distribution width), as large number of breakdown sites exist in the barrier layer per unit area. An analytical distribution function for V_C is followed by the PDM is given in Eq^N No. 9. The cumulative probability distribution of breakdown potential [$P(V_C)$], is presented in Eq^N No. 10 showing the percentage of all breakdown potential that are less than breakdown potential [31].

At varying pH (8.3, 9.3, 10.3) the potentiodynamic plots were carried out for 10 to 20 times to plot the cumulative probability distribution of breakdown potential as shown in figure 4.6. Calculated cumulative probabilities in the breakdown potential for type 304 stainless steel in borate buffer solution at pH=9.3 with different chloride concentration, compared with the experimentally determined distributions is shown in figure 4.13. The solid lines are the calculated distribution while the dotted lines are the experimental data.

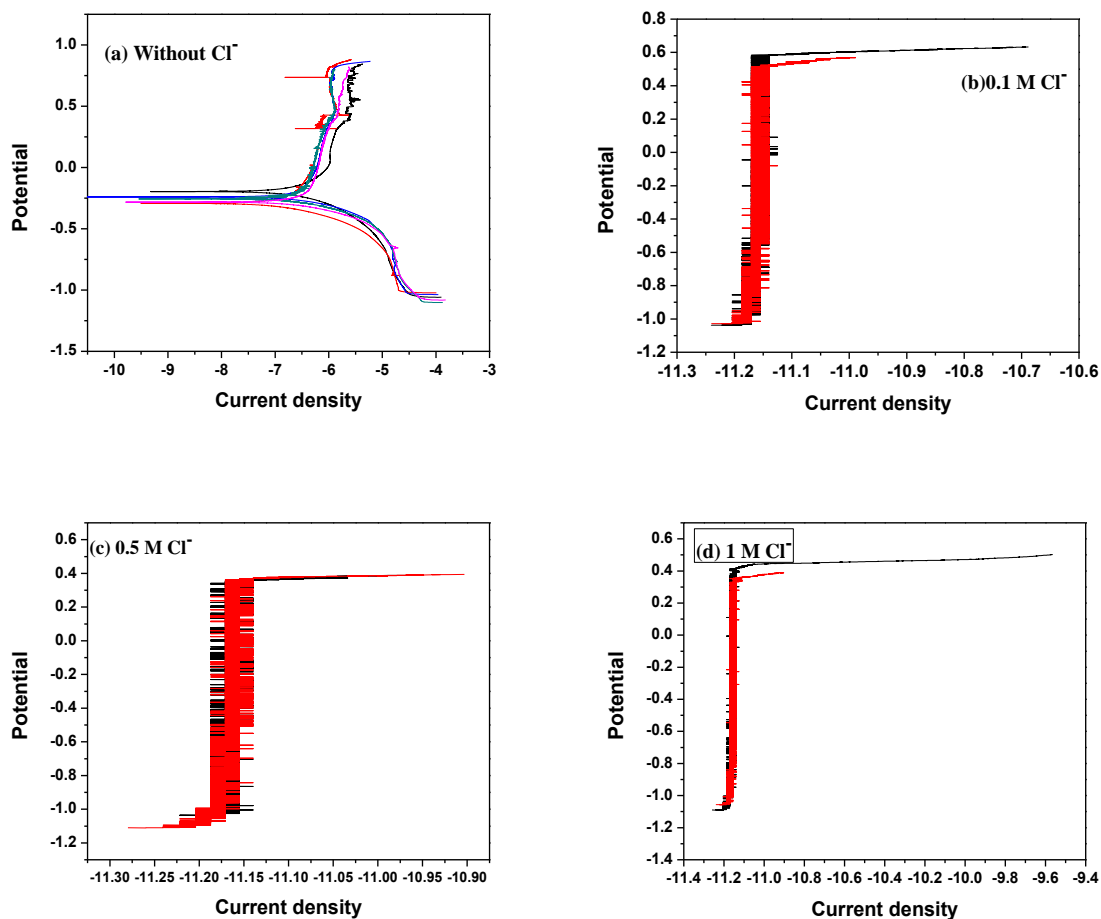
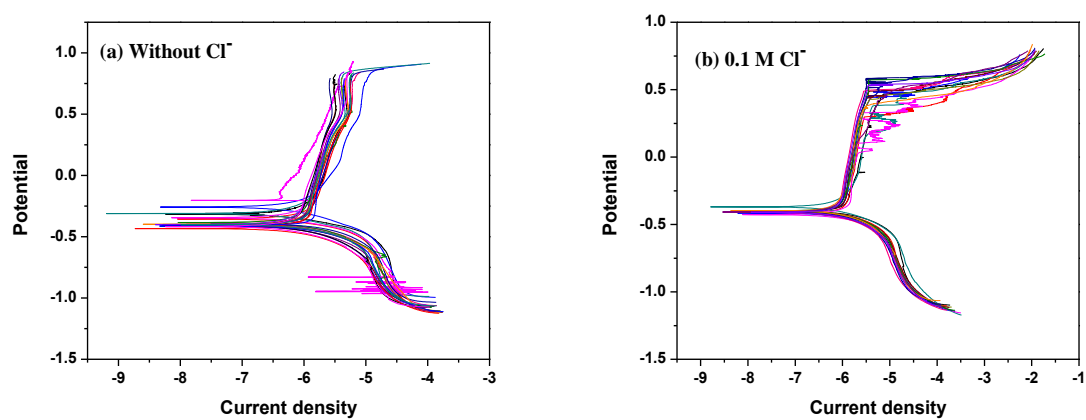


Fig 4.6:- Potentiodynamic curve at pH=9.3 with scan rate 0.167 mV/s



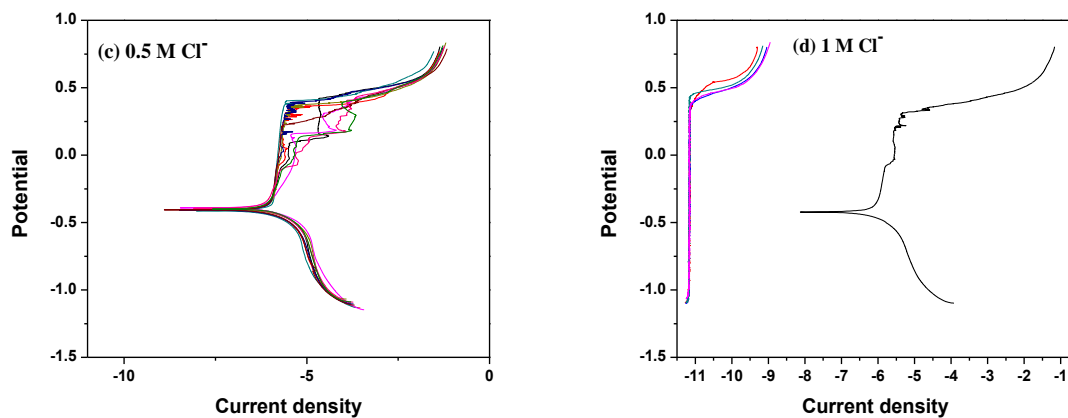


Fig 4.7:- Potentiodynamic curve at pH=9.3 with scan rate 1mV/s

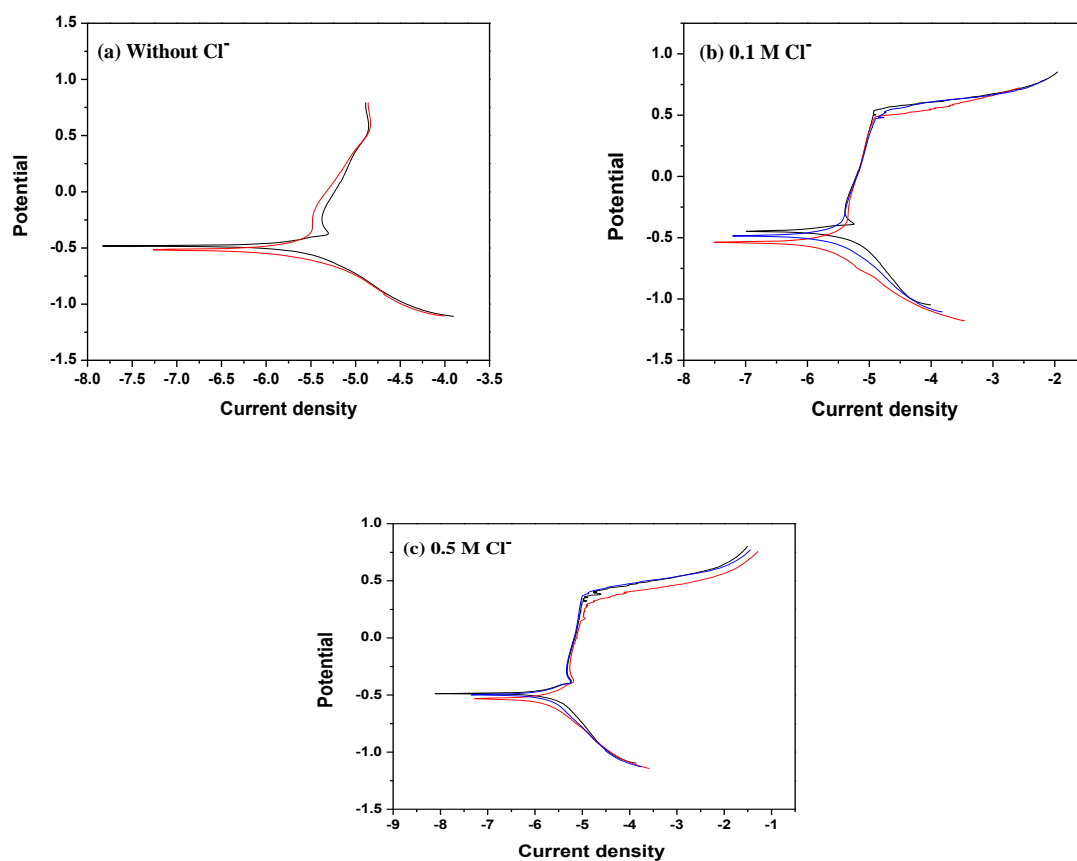


Fig 4.8:- Potentiodynamic curve at pH=9.3 with scan rate 5mV/s

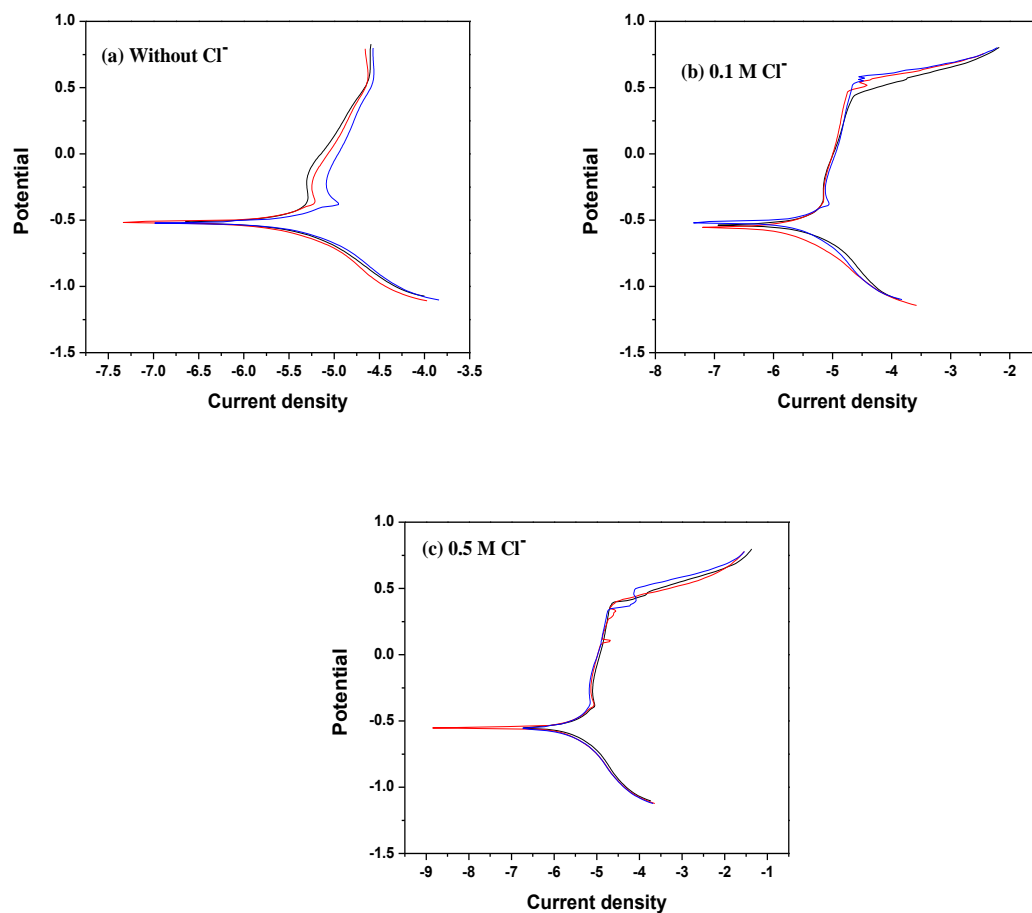
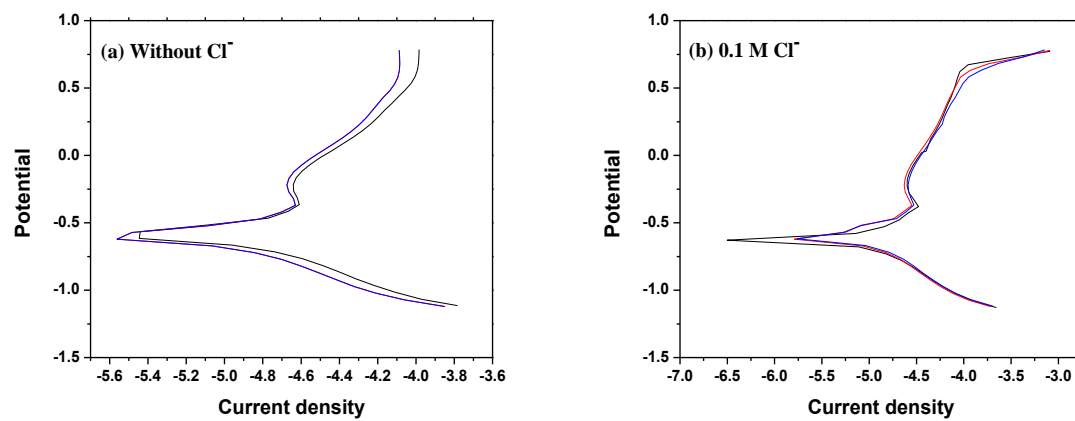


Fig 4.9:- Potentiodynamic curve at pH=9.3 with scan rate 10mV/s



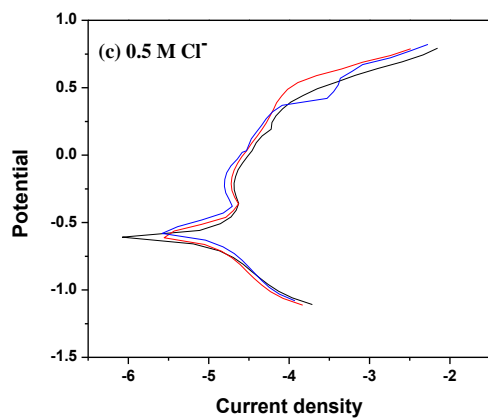


Fig 4.10:- Potentiodynamic curve at pH=9.3 with scan rate 50mV/s

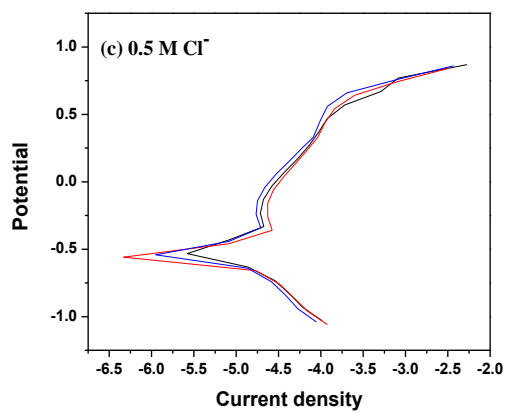
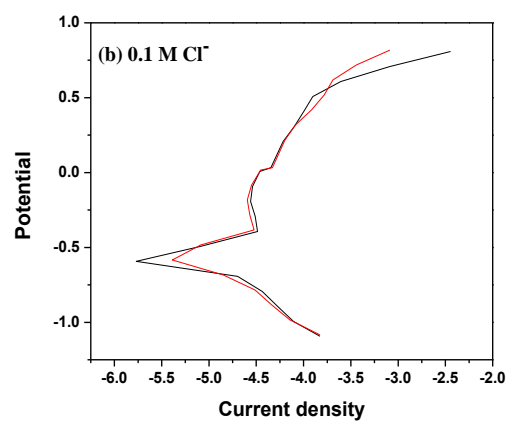
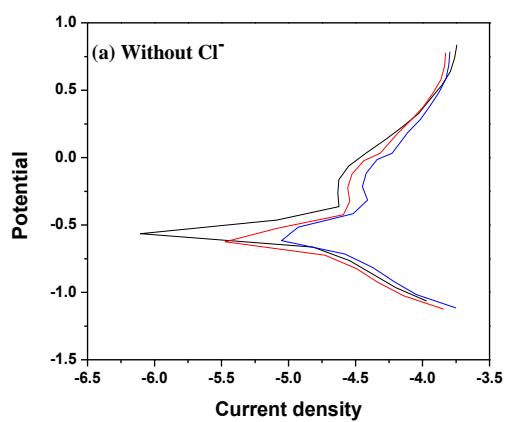


Fig 4.11:- Potentiodynamic curve at pH=9.3 with scan rate 100mV/s

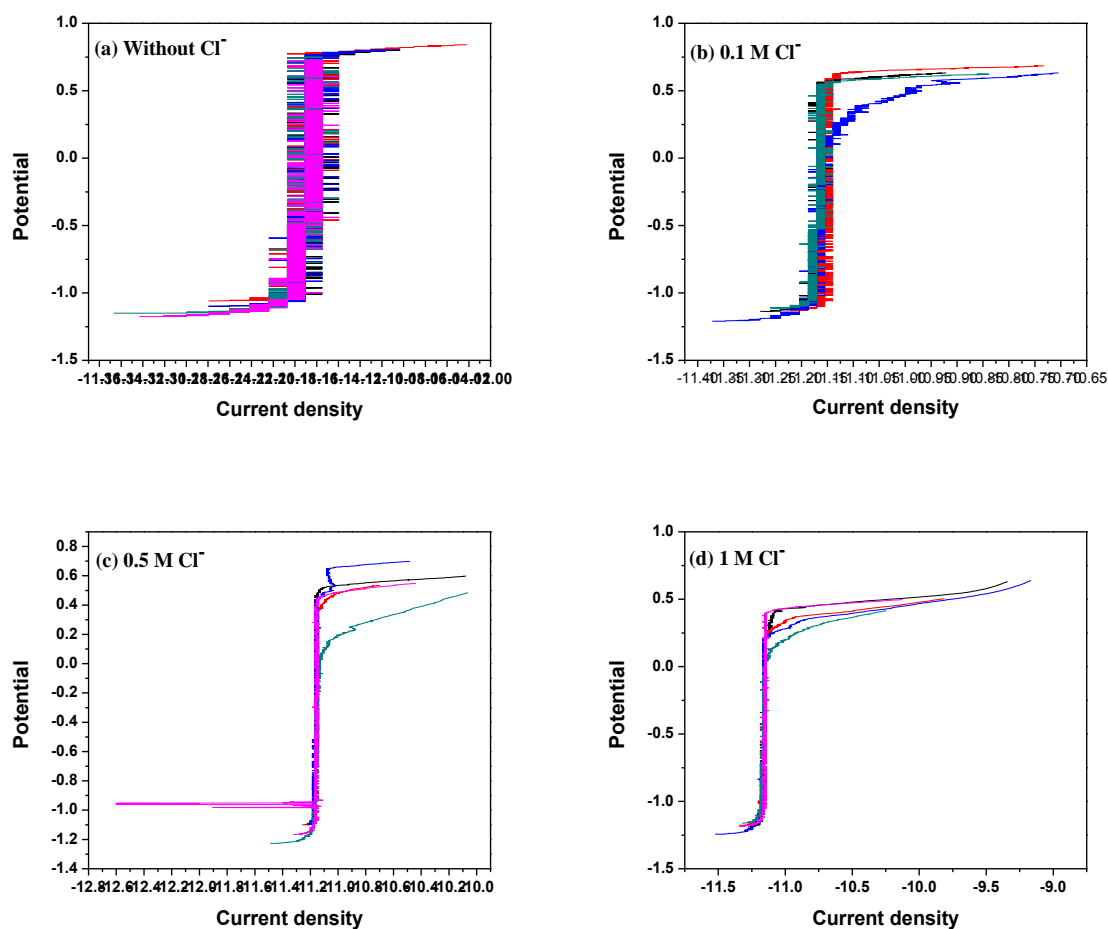


Fig 4.12:- Potentiodynamic curve at pH=10.3 with scan rate 1mV/s

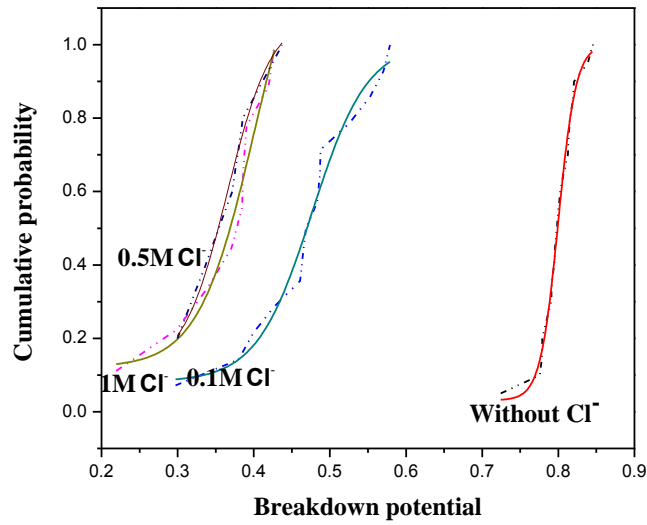


Fig. 4.13:- Cumulative probabilities in the breakdown potential for 304 SS with varying chloride concentration at pH 9.3

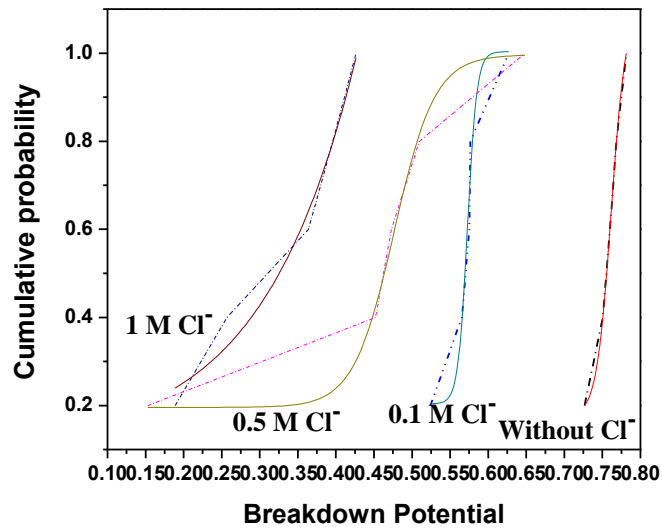


Fig. 4.14:- Cumulative probabilities in the breakdown potential for 304 SS in borate buffer solution with varying chloride concentration at pH 10.3

Parametrs	Value	Units
F, Faraday's constant	96487	C/mol
R, Gas constant	8.314	J/(mol K)
T, Absolute temperature	295	K
N _v , Avogadro's number	6.023×10 ²³	mol ⁻¹
χ, the barrier layer stoichiometry	3	
Ω, Molar volume per cation	14.59	cm ³ /mol
\bar{D} , The mean cation vacancy diffusivity	4×10 ⁻²⁰	cm ² /s
σ _D , Standard deviation for D	4×10 ⁻²⁰	cm ² /s
α, Potential dependence of $\Phi_{f/s}$	0.8	
ε, Electric field strength	5×10 ⁶	V/cm
ξ, Critical vacancy concentration	4.29×10 ¹⁴	no./cm ²
J _m , Critical vacancy flux	3.1×10 ¹²	no./(cm ² s)
β, pH dependence of $\Phi_{f/s}$	-0.01	V
$W = \frac{x}{2} \Delta G_A^0 + \Delta G_s^0 - \frac{x}{2} F \phi_s^0$	-29.235	kJ/mol

Table 4.1:- Parameters used to find the cumulative probabilities in breakdown potential

4.3 Microstructural analysis of pitting corrosion on 304 stainless steel

The microstructure of 304 stainless steel in borate buffer solution without chloride ion and with 1 M NaCl with varying is shown in figure 4.15. After adding the NaCl in buffer solution and maintain the pH by sodium hydroxide and then perform the experiment in potentiostat. The formation of the pits during the corrosion test are clearly visible in the microscope, which have taken from optical microscope. In the shape of the pit the corrosion parts are formed [34]. The pitting occurs in the stainless steel after adding NaCl in the buffer solution. Either stable or metastable pits can be form, it depends on the environmental conditions.

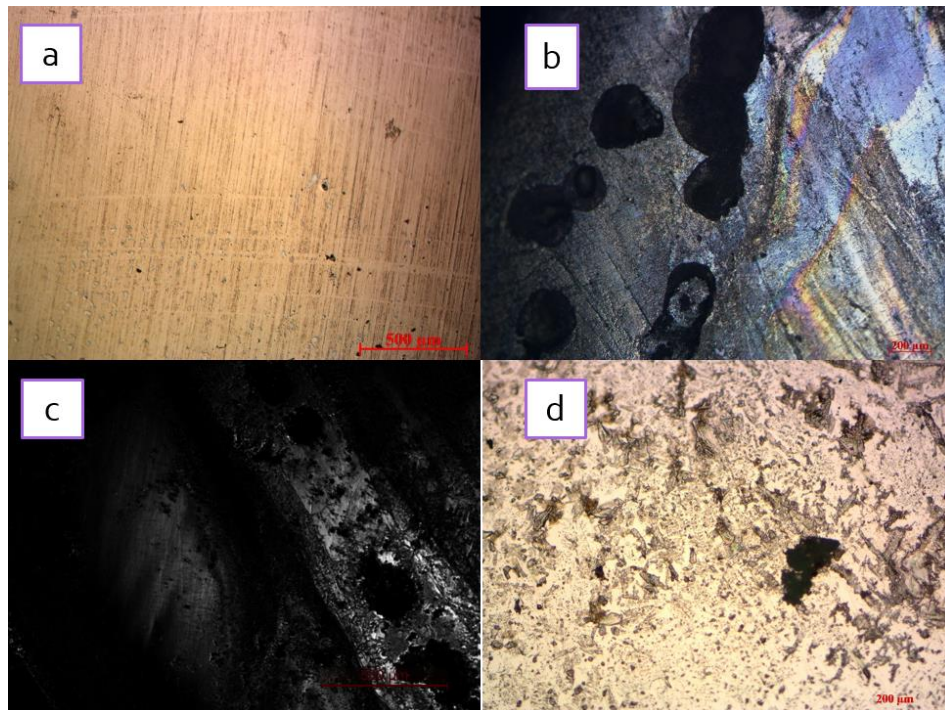


Fig. 4.15:- The microstructure of stainless steel before and after adding NaCl in solution

The microstructure of the steel after adding NaCl is showing in figure b, c, d and the pH values of the solutions were 8.3, 9.3, 10.3 respectively.

Chapter 5

Conclusion

5.1 Summary

In this topic the study concentrated on the passivity and passivity breakdown of 304 stainless steel in chloride containing borate buffer solution. The pitting corrosion is done on the surface of the 304 stainless steel at varying pH, potential scan rate and chloride concentration and microstructures are obtained from the optical microscope for the pitting corrosion.

- From the potentiodynamic plots the breakdown potential was obtained to decrease with increasing chloride concentration as predicted by the PDM. The behavior of breakdown potential was increased with increasing pH. And with increasing scan rate the breakdown potential increased.
- From the experiment, the passivation current density was not depend on the passivation potential.
- The relationships between breakdown potential and the pH, potential scan rate, and chloride activity find the parameters in according to the PDM for modelling the breakdown of passivity on 304 stainless steel. The breakdown potential dependencies on the chloride ion activity give the value of $\alpha = 0.8$, the polarizability of the film/solution interface.
- The PDM is then validated stating the fact that the nucleation and growth and the subsequent breakdown of the passive films is due to the point defects present in the film.
- The microstructures find from the optical microscope shows stable and metastable pits with corrosion products formed on the pits.

References

1. Mars G. Fontana, Corrosion Engineering, 3rd edition, 1987, p. 4.
2. Denny A. Jones, Principle and Prevention of Corrosion, 2nd edition, 1996, p. 11-19
3. Mars G. Fontana, Corrosion Engineering, 3rd edition, 1987, p. 39-41
4. Shimada, M., "Optimization of grain boundary character distribution for intergranular corrosion resistant 304 stainless steel by twin-induced grain boundary engineering." *Acta Materialia*, 50.6, 2002, 2331-2341.
5. Brown, S. A., and J. P. Simpson. "Crevice and fretting corrosion of stainless-steel plates and screws." *Journal of biomedical materials research*, 15.9, 1981, 867-878.
6. Reynolds, Anthony P. "Structure, properties, and residual stress of 304L stainless steel friction stir welds." *Scripta Materialia*, 48.9, 2003, p. 1289-1294.
7. Andresen, Peter L. "Effects of temperature on crack growth rate in sensitized type 304 stainless steel and alloy 600." *Corrosion* 49.9, 1993, p. 714-725.
8. Denny A. Jones, Principle and Prevention of Corrosion, 2nd edition, 1996, p. 199-203.
9. Mars G. Fontana, Corrosion Engineering, 3rd edition, 1987, p. 63-65.
10. Denny A. Jones, Principle and Prevention of Corrosion, 2nd edition, 1996, p. 209-220.
11. Strehblow, Hans-Henning, and Philippe Marcus. "Mechanisms of pitting corrosion." *Corrosion mechanisms in theory and practice*, 3rd edition, 1995, p. 201-238.
12. Strehblow, Hans-Henning. "Mechanisms of pitting corrosion." *Corrosion technology- New York and Basel-* 17, 2nd edition, 2002, p. 243-286.
13. Williams, D. E., C. Westcott, and M. Fleischmann. "Stochastic models of pitting corrosion of stainless steels I. Modelling of the initiation and growth of pits at constant potential." *Journal of the Electrochemical Society* 132.8, 1985, p. 1796-1804.
14. C. Chao and S. Smialowska, *Sur. Sci.*, 426, 1980, p. 96.
15. Macdonald, Digby D. "The history of the point defect model for the passive state: a brief review of film growth aspects." *Electrochimica Acta*, 56.4, 2011, p. 1761-1772.
16. Okamoto, Go. "Passive film of 18-8 stainless steel structure and its function." *Corrosion Science* 13.6, 1973, p. 471-489.

17. Zhang, Yancheng, Digby D. Macdonald. "Passivity breakdown on AISI Type 403 stainless steel in chloride-containing borate buffer solution." *Corrosion science*, 48.11, 2006, p. 3812-3823.
18. Macdonald, Digby D. "The point defect model for the passive state." *Journal of the Electrochemical Society*, 139.12, 1992, p. 3434-3449.
19. Urquidi-Macdonald, Mirna, and Digby D. Macdonald. "Theoretical distribution functions for the breakdown of passive films." *Journal of the Electrochemical Society*, 134.1, 1987, p. 41-46.
20. Hamadou, L., A. Kadri, and N. Benbrahim. "Characterisation of passive films formed on low carbon steel in borate buffer solution (pH 9.2) by electrochemical impedance spectroscopy." *Applied surface science*, 252.5, 2005, p. 1510-1519.
21. Frankenthal, R. P. "Passivation of iron in borate buffer solution." *Electrochimica Acta*, 16.11, 1971, p. 1845-1857.
22. Rao, Chepuri RK, and D. C. Trivedi. "Chemical and electrochemical depositions of platinum group metals and their applications." *Coordination Chemistry Reviews*, 249.5, 2005, p. 613-631.
23. Kose, Akira. "Direct observation of ordered latex suspension by metallurgical microscope." *Journal of Colloid and Interface Science*, 44.2, 1973, p.330-338.
24. Fattah-Alhosseini, A. "Effect of solution concentration on semiconducting properties of passive films formed on austenitic stainless steels." *Corrosion Science*, 52.1, 2010, p.205-209.
25. Cruz, RP Vera, Atsushi Nishikata, and Tooru Tsuru. "Pitting corrosion mechanism of stainless steels under wet-dry exposure in chloride-containing environments." *Corrosion science*, 40.1, 1998, p. 125-139.
26. Wilde, B. E., and E. Williams. "The use of current/voltage curves for the study of localized corrosion and passivity breakdown on stainless steels in chloride media." *Electrochimica Acta*, 16.11, 1971, p. 1971-1985.
27. Uhlig, Herbert H. "Passivity in metals and alloys." *Corrosion science*, 19.11, 1979, p. 777-791.
28. Sato, Norio. "A theory for breakdown of anodic oxide films on metals." *Electrochimica Acta*, 16.10, 1971, p. 1683-1692.
29. Lin, L. F., C. Y. Chao, and D. D. Macdonald. "A point defect model for anodic passive films II. Chemical breakdown and pit initiation." *Journal of the Electrochemical Society*, 128.6, 1981, p. 1194-1198.

30. Sato, Norio. "Anodic breakdown of passive films on metals." *Journal of the Electrochemical Society*, 129.2, 1982, p. 255-260.
31. Salvago, G., and G. Fumagalli. "Application of breakdown potential distribution in corrosion comparisons of stainless steels." *Corrosion*, 52.10, 1996, p. 760-767.
32. Drissi, S. H. "The preparation and thermodynamic properties of Fe (II) \square Fe (III) hydroxide-carbonate (green rust 1); Pourbaix diagram of iron in carbonate-containing aqueous media." *Corrosion science*, 37.12, 1995, p. 2025-2041.
33. Morales-Gil, P. "Corrosion inhibition of pipeline steel grade API 5L X52 immersed in a 1 M H₂SO₄ aqueous solution using heterocyclic organic molecules." *Electrochimica Acta*, 49.26, 2004, p. 4733-4741.
34. Chen, Y. Y. "Microstructure and electrochemical properties of high entropy alloys—a comparison with type-304 stainless steel." *Corrosion science*, 47.9, 2005, p. 2257-2279.